THE CELLULAR AND MOLECULAR BASIS OF NOXIOUS COLD DETECTION IN *DROSOPHILA MELANOGASTER* LARVAE

by

Kevin Armengol

A Thesis
Submitted to the
Graduate Faculty
of
George Mason University
in Partial Fulfillment of
The Requirements for the Degree
of
Master of Science
Biology

Committee:

_____	Dr. Daniel N. Cox, Thesis Director
_____	Dr. Giorgio Ascoli, Committee Member
_____	Dr. Karl J. Fryxell, Committee Member
_____	Dr. James D. Willett, Director, School of Systems Biology
_____	Dr. Donna M. Fox, Associate Dean, Office of Student Affairs & Special Programs, College of Science
_____	Dr. Peggy Agouris, Dean, College of Science
Date: _____	Spring Semester 2015 George Mason University Fairfax, VA

The Cellular and Molecular Basis of Noxious Cold Detection in *Drosophila melanogaster* Larvae

A Thesis submitted in partial fulfillment of the requirements for the degree of Master of Science at George Mason University

By

Kevin Armengol
Bachelor of Arts
University of Virginia, 2011

Director: Daniel N. Cox, Associate Professor
Neuroscience Institute, Georgia State University, Affiliate Faculty, School of Systems and Krasnow Institute for Advanced Study, George Mason University

Spring Semester, 2015
George Mason University
Fairfax, VA

DEDICATION

I dedicate this to my family, friends, and chinchillas (Monty and George) who all have been a constant source of support and inspiration throughout the years.

ACKNOWLEDGEMENTS

I would like to start off by thanking my various lab mates who contributed to this body of work: Luis Sullivan for getting the behavioral component of this work off the ground; Dr. Srividya Iyer, in particular for her valuable guidance and instruction on live imaging and the genetic and molecular techniques used in this work, as well as isolating genetic material for the comparative microarrays; Dr. Eswar Iyer for his assistance with the calcium imaging experiments and analysis; Surajit Bhattacharya for his contribution to the bioinformatics analysis of the microarray results; Atit Patel for his work with the cell isolation techniques and RT-PCR; and the rest of the Cox lab family for their ideas and support. I would also like to thank two of my committee members, Dr. Giorgio Ascoli and Dr. Karl Fryxell, for their invaluable guidance and instruction both in the classroom as professors and in the lab as committee advisors. Lastly, I would like to thank Dr. Daniel Cox for giving me the opportunity to work in his lab and being a constant source of encouragement and guidance in all aspects of this project. The lessons I learned from him, both inside and outside of the lab, have changed me forever, and in particular, have motivated me to pursue science even further and with an unrelenting passion. For that I am eternally grateful.

TABLE OF CONTENTS

LIST OF FIGURES

ABSTRACT

THE CELLULAR AND MOLECULAR BASIS OF NOXIOUS COLD DETECTION IN *DROSOPHILA MELANOGASTER* LARVAE.

Kevin Armengol, M.S.

George Mason University, 2015

Thesis Director: Dr. Daniel N. Cox

Nociception, the process of encoding and transmitting noxious stimuli within a nervous system, is an essential mechanism through which organisms are alerted to potentially life-threatening insults or conditions that originate externally or internally and may lead to incipient tissue damage. These insults can be classified into three broad types of stimuli: chemical, mechanical and thermal. Despite significant progress in this field of study, our understanding of the neural bases of noxious cold detection remains poorly understood. The *Drosophila melanogaster* larval peripheral nervous system (PNS) has emerged as an excellent model system for studying both the cellular and molecular mechanisms of nociception, particularly with regards to noxious heat and mechanical stimuli. Using this model system, we have implemented a systems neuroscience approach to dissect the underlying cellular, genetic, molecular, and behavioral bases of noxious cold detection. We have developed the first behavioral assay for investigating cold nociception in *Drosophila* and have identified unique noxious cold-evoked behavioral responses. These cold-specific behaviors require synaptic

transmission predominantly from class III dendritic arborization (da) sensory neurons. Optogenetic activation of class III neurons, independent of thermal stimulation, is sufficient to behaviorally phenocopy noxious cold-evoked behavior. Moreover, GCaMP6 functional analyses reveal specific activation of class III da neurons in response to noxious cold stimulation. At a molecular level, microarray analyses revealed these neurons are enriched with a broad spectrum of ion channels, including numerous Transient Receptor Potential (TRP) channels. Mutant and cell-type specific RNAi analyses reveal that select TRP channels *Trpm, nompC* and *Pkd2* are required for normal cold-evoked behaviors and function in the transduction step of noxious cold stimulation. Collectively, our results establish a novel systems-level framework for exploring cellular and molecular mechanisms underlying thermosensory nociception.

INTRODUCTION

Nociception, the process of encoding and transmitting noxious stimuli within the nervous system, is an essential mechanism through which organisms are alerted to potentially life-threatening insults or conditions that originate externally or internally[1–5] . Noxious mechanical, thermal, and chemical stimuli are transduced by specialized, high threshold peripheral nociceptors whose firing is often coupled with a reflexive behavior, change in motivational state, and/or the conscious perception of pain; these responses all aid in removing the organism from the source of danger or injury[6–9]. While the detection of noxious stimuli is necessary for organismal survival and success, there are many situations in which nociception and the resulting feeling of pain are undesirable or even maladaptive. For instance, the medical community relies heavily on the use of anesthetics and analgesics to dull or eliminate a patient's nociception and pain in order to perform various surgical procedures or provide temporary relief of acute symptoms. Many patients also suffer from chronic and sensitized forms of pain as a result of complex pathophysiological processes involving inflammation, peripheral or central nervous system damage, and/or genetics[10–13].

Chronic pain can roughly be categorized into two kinds: nociceptive and neuropathic. Nociceptive pain is the result of nociceptor activation due to injury and examples include post-operative pain and sports injuries. Neuropathic pain is the result of damage to or malfunction of the central or peripheral nervous system (including nociceptors) and examples include trigeminal neuralgia, complex regional pain syndrome

(CRPS) and phantom limb pain[14]. Some conditions, such as arthritis, straddle both the nociceptive and neuropathic pain categories[15]. Generally, this dichotomous distinction can guide treatment as nociceptive pain is more responsive to opioid and non-steroidal anti-inflammatories (NSAIDS) treatment, whereas neuropathic pain is more responsive to tricyclic antidepressants (TCA), local anesthesia, and anticonvulsants[16]. However, for numerous patients suffering from neuropathic pain, prescribed treatments often fail to relieve their symptoms, become less effective with time, or come with a host of unwanted side effects. These observations are, in part, due to the heterogeneous nature of chronic pain, with multiple distinct etiologies that have the ability to evolve with time due to the phenomena of neuroplasticity.

Symptoms of chronic pain are quite heterogeneous as well, with patient descriptions including words like: "shooting," "tingling," "aching," "burning," and/or "freezing." The latter two descriptions, "burning" and "freezing," highlight one common manifestation of chronic pain, altered noxious thermosensation. In mammals, noxious thermal stimuli are transduced by high threshold thermosensitive ion channels located in the sensory endings of a subset of peripheral Aδ (myelinated) and C (non-myelinated) fibers; processing of this information occurs in the spinal cord and brain[17].In many chronic pain states, it appears this thermal nociceptive circuitry is malfunctioning, causing the patient to feel the presence of noxious thermal stimuli despite its absence. Interestingly, there has been accumulating evidence that targeting the canonical noxious heat transducer, Transient Receptor Vanillin 1 (TRPV1), with antagonists can alleviate pain in patients. This represents a unique approach to pain relief as most drugs target the

inflammatory system and propagation and transmission of the signal to the spinal cord[18]. Unfortunately, side effects of this class of drugs can include impaired noxious heat sensation, shivering, and hyperthermia. Recently, it has been shown that there exists a dynamic balance between hot and cold neural circuitry that may be responsible for these unwanted side effects of TRPV1 antagonists[19]. Both the failure and success of this treatment though suggests that elucidating the cellular and molecular mechanisms that regulate thermal nociception may be critical in identifying and implementing novel strategies for the treatment of chronic pain[20]

Although the basic mechanisms for detecting noxious heat are fairly well understood, those underlying noxious cold perception are less clear. Recently, the model system, *Drosophila melanogaster,* has been successfully used to identify key conserved molecules and mechanisms in both thermal (heat) and mechanical nociception and nociception sensitization[21–24].The advantage of using a genetically tractable system like *Drosophila* to study cold nociception is that it allows unbiased forward genetic analysis in a feasible and cost effective manner. The few cold studies performed to date in *Drosophila,* however, have focused on thermal preference in ambient or innocuous cool temperature ranges, so noxious cold detection is relatively unexplored territory. In fact, larval responses to noxious cold have not yet been reported in the literature. Furthering our understanding of the cellular and molecular mechanisms of cold nociception with this model may ultimately lead to successful therapies for certain chronic pain conditions and may possibly address the side effects of TRPV1 antagonist treatment.

1.1 *Drosophila* da neurons as a model system

The *Drosophila* larvae PNS has emerged as a powerful model organism to study the cellular and molecular mechanisms underlying nociception[25–27] and thermosensation[28–30]. In larvae, two major types of sensory neurons innervate the epidermis **(Fig.1)**: type I neurons, with a single ciliated dendrite; and type II neurons, with multiple dendrites, also known as multidendritic (md) neurons. A subset of md neurons, known as dendritic arborization (da) neurons, have characteristic naked dendritic projections to the epidermis similar to vertebrate nociceptors[31,32]. There are four classes of da neurons (CI-CIV), each with their own unique morphology and sensory role **(Fig.2)**. Previous studies have implicated a subset of da neurons, CIVs, as being the primary responders to noxious heat and noxious mechanosensation[23,33–35].

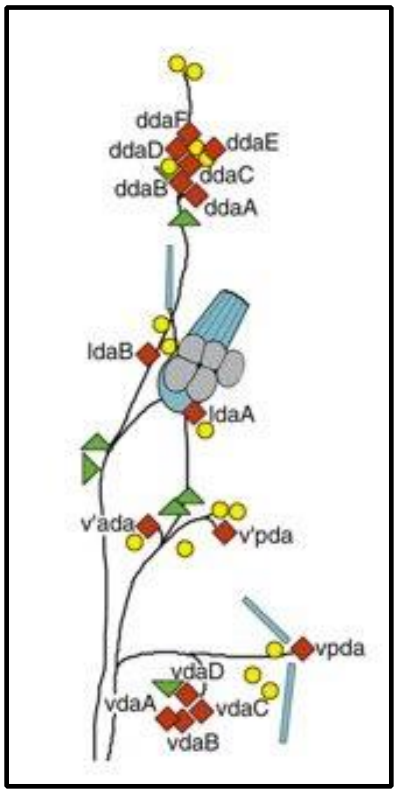

Figure 1. Drosophila abdominal PNS. Schematic depicts a single abdominal hemisegment in which da neurons are denoted as red diamonds. Hemisegmental da neuron clusters include dorsal, lateral, ventral', and ventral, present within the dorsal, lateral and ventral regions respectively, and are denoted by the prefixes d, l, v', and v. Figure reproduced from Grueber et al., (2002)[36].

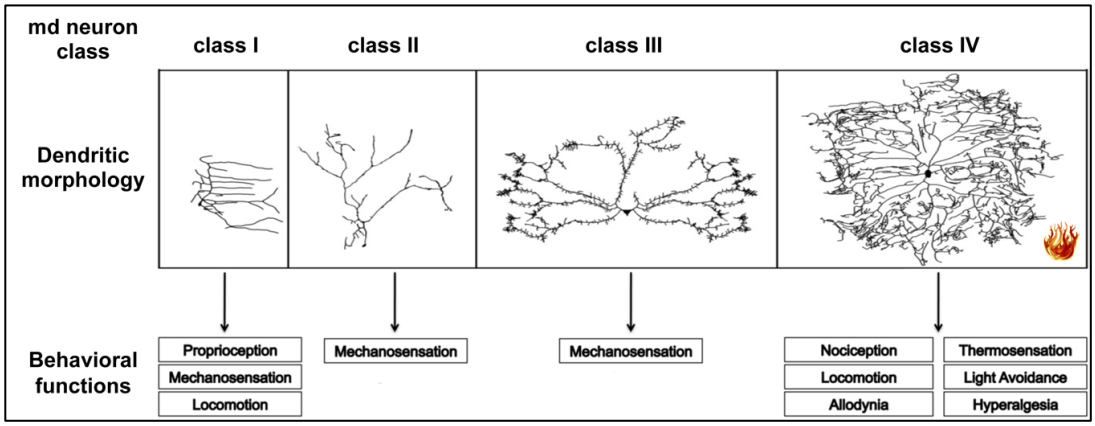

Figure 2. *Drosophila* da neurons. Larval da neurons exhibit class-specific dendritic morphologies and contribute to distinct sensory and nociceptive behavioral responses**.**

1.2 TRP channels

Transient receptor potential (TRP) channels are part of a multigene superfamily that encodes ion channels. The TRP family is subdivided into seven subfamilies: TRPC (canonical), TRPV (vanilloid), TRPM (melastatin), TRPP (polycystin), TRPML (mucolipin), TRPA (ankyrin) and TRPN (NOMPC-like); the latter of which is only found in invertebrates and fish. They contain multiple subunits, six transmembrane domains, and conduct cations with varying degrees of selectivity. Diverse TRP channels are intimately involved in all sensory modalities, including various types of nociception[37–39]. For instance, in vertebrates, TRPV1 responds to noxious heat stimuli in the skin[40] and in flies painless is required for aversive rolling to both harsh touch and high temperatures[33]. However, the cells and channels required for responding to cold have been more difficult to pinpoint. TRPM8 responds to innocuous cool temperatures in the vertebrate skin[41]. Moreover, TRPM8 detects both innocuous and noxious cold in rat DRG neurons[42]. TRPA1 has also been implicated as a vertebrate noxious cold receptor[43], however there are cold sensing neurons that do not express TRPM8 or TRPA1[44,45], suggesting that there are other yet unidentified channels involved in noxious cold sensing. This is also evidenced by the fact that TRPM8 KO animals still show a sensitivity to noxious cold independent of TRPA1[46]. The few cold studies performed to date in *Drosophila* have focused on thermal preference in ambient or innocuous cool temperature ranges and have yielded promising results for TRP channels in sensing cool temperatures. *trp* and *trpl* are required for cool avoidance (10-20°C) in larvae[47] and *brivido*, a channel similar to TRPP, is involved in sensing cool temperatures in the range of 12-15°C in adult flies[29]. Although

TRP channels are clearly involved in cool avoidance in *Drosophila*, whether they play a role in any responses to acute noxious cold has yet to be investigated. **Figure 3** shows our current understanding of the thermosensory role various TRP channels play in *Drosophila.*

TRP Family	TRP Channel	Thermal Function
TRPC	TRP	Cool avoidance
	TRP gamma	Unknown
	TRPL	Cool avoidance
TRPM	TRPM	Unknown
TRPN	NOMPC	Unknown
TRPV	NAN	Unknown
	IAV	Unknown
TRPA	TRPA1	Chemical, thermal preference, thermal hyperalgesia
	pyrexia	Noxious heat
	painless	Noxious heat, thermal allodynia
	WTRW	Unknown
TRPP	PKD2/AMO	Unknown
	BRV1	Cool avoidance
	BRV2	Cool avoidance
TRPML	TRPML	Unknown

Figure 3. TRP channel thermal functions.

1.3 GAL4-UAS system

The *GAL4-UAS* system was first discovered in yeast, *Saccharomyces cerevisiae,* as a regulator of genes induced by galactose. The system comprises a transcriptional activator protein, GAL4, with DNA binding activity that targets a specific DNA sequence known as the Upstream Activating Sequence (UAS), an element similar to enhancers in multicellular eukaryotes. Once the GAL4 protein binds to the UAS sequence, transcription of genes downstream of the UAS sequence can occur[49].

The *GAL4-UAS* system has been coopted in numerous model systems to aid in targeted gene expression. In *Drosophila,* transgenic expression of UAS constructs can be precisely controlled both spatially and temporally with the use of enhancer traps that place the GAL4 under the regulatory control of cell-specific enhancers **(Fig.4)**.

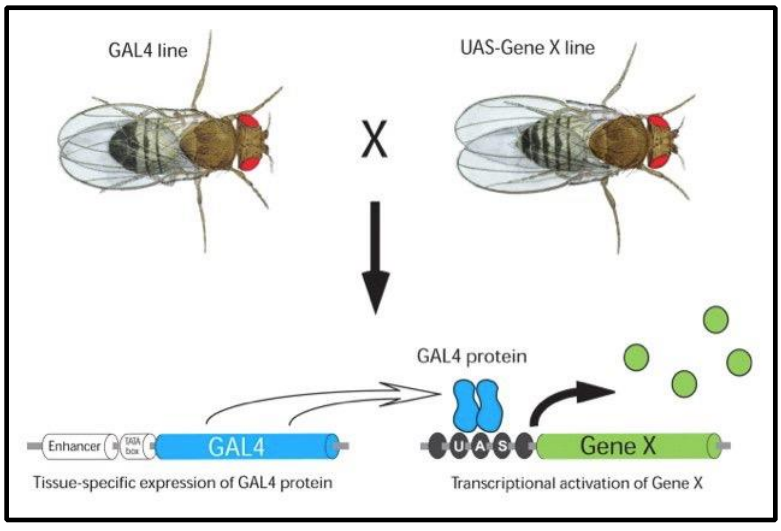

Figure 4: *GAL4-UAS* system in *Drosophila*. Adult flies carrying a *GAL4* driver are mated to flies carrying a *UAS* construct (i.e. *UAS-mCD8::GFP*) to produce progeny containing both constructs. This results in the activation of Gene X in a tissue-specific manner. Image reproduced from Southall, Elliott, & Brand (2008)[50].

1.4 Preliminary Studies

Drosophila larvae contract in response to noxious cold

To determine if *Drosophila* larvae produce a behavioral response to noxious cold, we developed a novel cold plate assay for global stimulation of larvae with noxious cold temperatures **(Fig.5A)**. Three distinct behaviors were observed in wild-type larvae to varying degrees as a function of temperature (4-16˚C): abnormal locomotive crawling; head and/or tail raise (HTR); and a forceful, fully-body contraction (CT) along the antero-posterior axis **(Fig.5B)**. CT behavior is non-existent above 16˚C, but dominates the larval response at temperatures <10˚C, maximizing at 4-6˚C. HTR behavior is maximal at 10˚C. Abnormal crawling locomotion dominates at temperatures >14˚C. The results from this assay indicate that *Drosophila* larvae exhibit a unique set of behaviors in response to noxious cold that are distinct from normal locomotion, light touch responses[51], and aversive rolling to noxious heat or mechanical stimuli[33]. These easily identifiable behaviors serve as a platform to probe the cellular and molecular bases of noxious cold detection in *Drosophila* larvae.

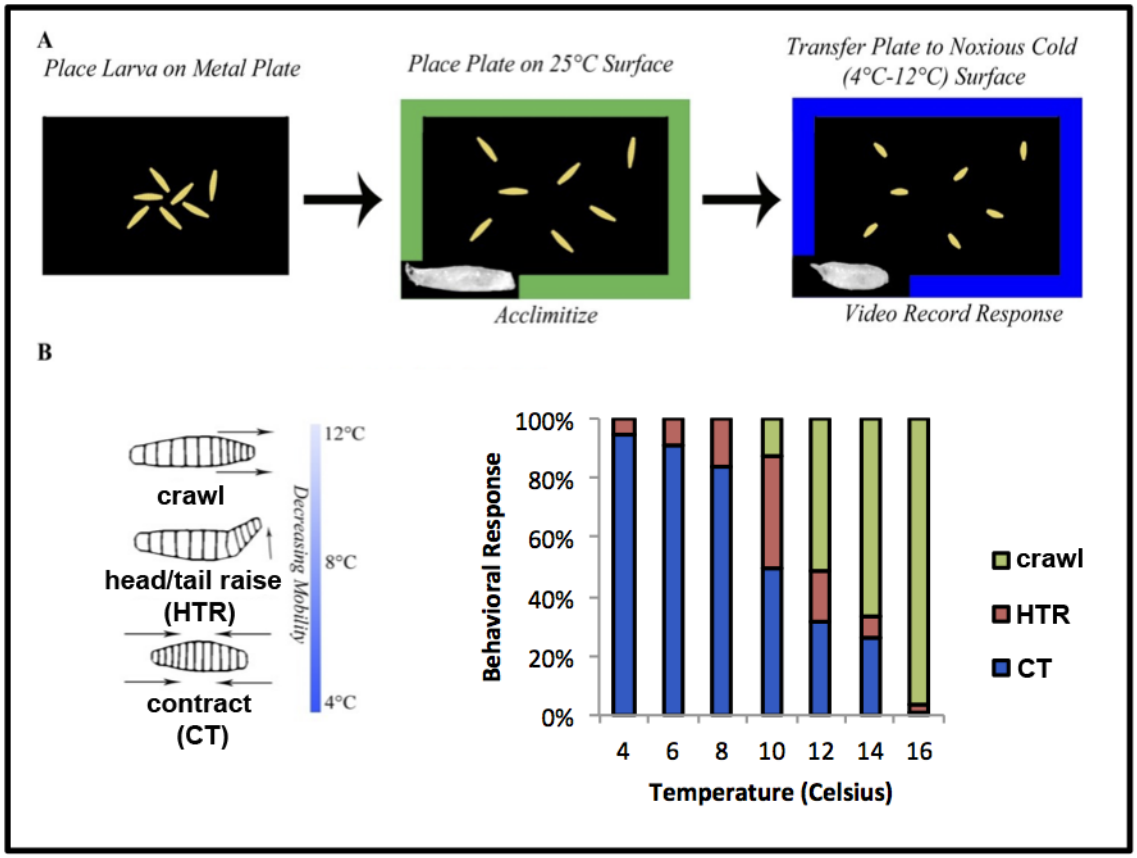

Figure 5. Cold plate assay procedure and behaviors as a function of temperature

(A). Larva are placed on a thin metal surface and allowed to acclimatize to a 25˚C surface. The plate is then transferred, without touching the larvae, to another surface of variable temperature (4˚-12˚C). (**B)** As temperature decreases, crawling and head/tail raise (HTR) behaviors are replaced by the contract (CT) response.

Specific Aims:

AIM 1a: To identify the cellular basis of cold nociception in *Drosophila melanogaster* larvae.

Hypothesis: Given previous findings of a subset of da neurons involved in nociception, we hypothesized that one or more da neuron subtypes are required for cold nociception.

Approach: We systematically blockaded neural transmission by inhibiting synaptic release in identifiable subsets of da neurons *in vivo* through targeted expression of tetanus toxin coupled to the cold plate assay. These analyses were complemented by parallel optogenetic studies in order to determine which behaviors result as a function of da neuron subtype stimulation. Additionally, da neuron activity were monitored *in vivo* with the GCaMP6 calcium reporter under normal and noxious cold conditions to assess which neurons respond specifically to noxious cold stimulation.

AIM 2: To identity molecular pathways that mediate cellular sensitivity to noxious cold stimuli.

Hypothesis: Given the role of TRP channels in mediating various types of nociception in invertebrate and mammalian systems, it is likely one or more TRP channels govern cellular sensitivity to noxious cold stimuli.

Approach: A comparative microarray was conducted between putative cold nociceptors and noxious cold insensitive neurons to determine upregulated ion channels in the former. Once these upregulated channels were identified, we utilized various RNAi and

mutant constructs to alter channel number, function, or presence, and conducted our cold plate assay.

Research Plan:

AIM 1a: To identify the cellular basis of cold nociception in *Drosophila melanogaster* larvae.

Synaptic Inhibition:

The tetanus toxin construct *UAS-TNTE* was expressed in a class-specific manner using the following GAL4 drivers*: GAL4*^{221} (CI), *GAL4* $^{\text{GMR37B02}}$ (CII), *GAL4*^{CIII} (CIII), *GAL4*$^{19\text{-}12}$ (CIII), *GAL4*^{nompc} (CIII), *GAL4*$^{1003.3}$ (CII/CIII), and *GAL4*$^{477;ppk}$ (CIV). As a control, an inactive form of the tetanus toxin was expressed using *UAS-IMP-TNTA* with the same drivers. The cold plate assay was conducted at 6˚C to maximize the potential CT response and avoid the quick onset of relaxation observed post-CT behavior at 4˚C. Larval change in body length was videotaped then quantified using NIH's ImageJ image processing software. During analysis, larvae that did not exhibit HTR or crawling defects were categorized as a CT responder if they fell within 1.5 SD of the average change in body length for wild-type larval controls.

Optogenetic Activation:

The light sensitive ion channel ChETA was expressed in a class-specific manner using *UAS-CHETA-YFP* in conjunction with the following GAL4 drivers: $GAL4^{221}$ (CI), $GAL4^{GMR37B02}$ (CII), $GAL4^{19\text{-}12}$ (CIII), and $GAL4^{477;ppk}$ (CIV). Larvae were supplemented with the essential co-factor *all-trans*-retinal necessary for ChETA function as they lack it naturally (except in the negative controls). Larvae were stimulated globally, one at a time, using 480nm light under a stereomicroscope. Larval behaviors were videotaped then analyzed qualitatively by the experimenter as well as quantitatively using NIH's ImageJ image processing software.

Calcium Imaging:

The genetically encoded calcium indicator, GCaMP6, was expressed in all da neurons using the *UAS-GCaMP6* transgenic construct in conjunction with the pan-da driver $GAL4^{217\text{-}RFP}$. Live animals were fixed between a coverslip and a microscope slide and placed on top of a thermo-controlled peltier plate. Using live confocal imaging, the calcium signals from dorsal surface da neurons were analyzed simultaneously under various surface temperature conditions ranging from 25˚C to 6˚C. Calcium signals were analyzed using NIH's ImageJ image processing software.

AIM 2: To identity molecular pathways that mediate cellular sensitivity to noxious cold stimuli.

Once a potential cold nociceptor and non-cold nociceptor were identified, comparative microarray analyses and RT-PCR validation were performed to assess differential mRNA transcript expression across da neuron subtypes. We hypothesized that channels that are upregulated in cold nociceptive cells may be responsible for cell-type specific sensitivity to noxious cold.

Behavioral Analysis:

Once potential channels were identified, various RNAi, mutant, and deficiency lines were obtained, and larvae expressing them were subjected to the cold plate assay to assess their impact on CT behavior. Class specific rescue experiments were performed for mutants showing CT deficits. Additionally, a functional optogenetic analysis was conducted to assess whether or not these channels function at the transduction stage or propagation stage.

EXPERIMENTAL PROCEDURES

Fly Strains and Genetics

Drosophila melanogaster larvae were raised on cornmeal food at 25°C. *Oregon R* was used as a control strain. Mutants: *Pkd2*$^{1(52)}$, *TRPM*, *nompC*. Deficiencies: *Df(2L)BSC407* (*Pkd2*), *Df(2R)XTE-11* (*Trpm*), and *Df(2L)Exel6012* (*nompC*). Gal4 Lines: *GAL4*$^{2\text{-}21}$ (class I[34]), *GMR37B02-GAL4* (class II[53]), *19-12-GAL4* (class III[54]), *nompC-GAL4* (class III[55]), and *GAL4*$^{ppk1.9}$*,ppk-GAL80* (class III[56]), *GAL4*$^{ppk1.9}$ and *GAL4*^{477}*;GAL4*$^{ppk1.9}$ (class IV[56,57]), *1003.3-GAL4* (class II and III[58]), and *GAL4*$^{21\text{-}7}$ (classes I-IV[59]). UAS transgenes: *UAS-TeTxLC* (*TNT-E*) (active tetanus[60]), *UAS-IMP TNT VI-A* (inactive tetanus[60]); *UAS–GCaMP6m*$^{(61)}$; *UAS-channelrhodopsin-2* (ChETA-YFP[55]); *UAS-mCD8::GFP*. *UAS-RNAi* lines targeting the indicated genes: From Vienna Drosophila RNAi Center: 6941 *(UAS-Pkd2*^{RNAi}*)*; from Bloomington Drosophila Stock Center at Indiana University: 31296 (*UAS-Pkd2*^{RNAi}), 31675 (*UAS-Pkd2*^{RNAi}), 31672 (*UAS-Trpm*^{RNAi}), 35581 (*UAS-Trpm*^{RNAi}), 33670 (*UAS-Trpm*^{RNAi4}), 31689 (*UAS-nompC*^{RNAi}), and 31512 (*UAS-nompC*^{RNAi}). Stocks used for rescue: *UAS-Pkd2*$^{(62)}$ (gift of Xiang Lu), *UAS-nompC.L-GFP*$^{(63)}$ (gift of Yuh Nung Jan). Stocks used for structure-function studies: *UAS-Rac1.N17*$^{(64)}$; *UAS-nompC.* Δ*12ANK-GFP*$^{(63)}$*; UAS-nompC.* Δ*29ANK-GFP*$^{(63)}$ (gift of Y.N.J.).

Global cold plate assay

To determine behavioral responses to whole body global cold stimulation, mid third instar larvae were placed on a 25°C thin, black metal plate (2 mm) coated with a fine mist of water. Once larvae acclimated and initiated peristaltic locomotion, the metal plate was gently transferred (without touching the larvae) to a peltier-controlled plate pre-set to a specific temperature (4˚C – 16˚C). The cold plate design allowed contact with the entire ventral surface of the larva. Cold plate temperature uniformity was verified with a Fluke 62 mini infrared thermometer independent of the digital readout on the cold plate. Response to noxious cold was video recorded for 45 seconds at 5 fps. Initial behavioral responses within the first 5s of stimulation were scored through a combination of qualitative and quantitative measures. Behaviors such as crawling and head and/or tail raise were scored qualitatively by the experimenter and designated "crawling" and "HTR," respectively. If larvae did not fall into these two classes they were subjected to quantitative analysis. This consisted of measuring their change in body length using the Skeletonize and Analyze Particles functions in Image J. Larvae were categorized as "contraction responders" (CT) if the maximum percent change in body length exceeded a threshold value of 1.5 standard deviations below the average maximum percent change in length for wildtype larvae. Larvae who failed to exceed the threshold were subsequently categorized as "non-responders" (NR). Larvae were discarded if they were not fully extended upon placement of the plate on the cold plate and each larva was only stimulated once at a given temperature. Data was expressed as the percentage of behaviors exhibited per condition and statistically compared to appropriate controls using

Fisher's exact test with a Bonferonni correction. As 6˚C was found to elicit a strong CT response in wildtype larvae, subsequent cold plate assays with mutants or class-specific RNAi were performed at 6˚C.

***in vivo* calcium imaging**

GAL4^{217},UAS-mCD8::RFP (pan da GAL4) or *19-12-GAL4,UAS-mCD8::RFP* (CIII) was used to drive the genetically encoded calcium indicator *UAS-GCaMP6* (medium variant). Live, unanesthetized mid third-instar larvae were individually placed on a glass microscope slide and immobilized by placing a 22x50 mm glass coverslip on top of the larvae; the glass coverslip was supported at both ends by a smaller 22x22mm glass coverslip so as not to compress the larvae. The microscope slide preparations were placed on a Linkam PE 120 peltier stage and clamps were placed on top of the coverslip to fully immobilize the larva. The Linkam PE 120 stage was placed underneath a Nikon C1 Plus confocal microscope equipped with a 20x oil immersion lens for larval imaging. Each larva was individually subjected to a temperature regiment programmed via the Linkam T95 controller. The temperature regiment for pan da GAL4 GCaMP6 (m) expression was as follows: an initial 300s of 25^{o}C, a ramp down to 6^{o}C at a rate of 20.0^{o}C/min, a hold at 6^{o} for 10s, a ramp up to 25^{o}C at a rate of 20.0^{o}C/min, and a final hold at 25^{o}C for 120s. The temperature regiment for CIII GCaMP(m) expression was as follows: an initial 120s of 25^{o}C, a ramp down to 6^{o}C at a rate of 20.0^{o}C/min, a hold at 6^{o} for 10s, a ramp up to 25^{o}C at a rate of 20.0^{o}C/min, a hold at 25^{o}C for 60s, a ramp down to 6^{o}C at a rate of 20.0^{o}C/min, a hold at 6^{o} for 10s, a ramp up to 25^{o}C at a rate of

20.0°C/min, and a final hold at 25°C for 60s. Dorsal da neuron clusters were visualized during each temperature regiment with 256x256 resolution and videos were taken at a frame interval of 620ms. During analysis, videos were motion corrected using the Image J plugin *StackReg*[65]. Videos with excessive larval movement were discarded. Mean fluorescence of the neuronal soma for a given cell-type was measured using Image J's plot z-profile function. Data was smoothed with a 5 frame moving average in the statistical programming language *R*. $\Delta F/F_0$ X 100% was calculated for each frame with F being the fluorescence intensity at a given frame and F_0 being the average baseline fluorescence at 25° C for 300s prior to the ramp in the pan da condition and 30 frames prior to each ramp down to 6° C in the CIII condition. Max $\Delta F/F_0$ was calculated for each ramp down to 6° C and averaged amongst all larvae. Mann-Whitney U-tests were used to calculate differences in average $\Delta F/F_0$ between da neurons. For cross-correlation analyses, correlation coefficients (product-moment coefficient of correlation – Pearson's correlation) were calculated in Microsoft Excel® to examine the maximum correlation value between an individual neuron's GCaMP6 signal and the corresponding temperature signal. A negative correlation indicates that as temperature declines, GCaMP6 fluorescence increases.

Optogenetics

Third instar larvae, expressing the ultrafast channelrhodopsin-2 variant transgene *UAS-CHETA-YFP*[55] under the control of da neuron class-specific *GAL4* drivers (CI, CII, CIII, or CIV), were activated with blue light exposure to assess the impact of class-

specific neuronal activation on behavioral output. Simultaneous optogenetic activation of CIII and CIV da neurons was achieved by crossing CIII-specific *19-12-GAL4,UAS-CHETA::YFP* recombinant flies to CIV-specific $GAL4^{477};GAL4^{ppk1.9}$ flies, and resultant larval progeny bearing YFP expression in both CIII and CIV neurons were behaviorally analyzed. Larvae were reared in the presence or absence of 1500 micromolar all *trans*-retinal (ATR) from the first larval instar (~24 hours after egg laying) and were subjected to optogenetic activation at the third larval instar using the Hg light source of a Leica MZ16 FA stereomicroscope (14,500 lux). The stimulation regiment consisted of three successive 5 second pulses of blue light (480nm) separated by 10 second periods with no blue light stimulation. Videos of behavioral responses were recorded with a Nikon D5000 DSLR camera mounted on the Leica MZ16 FA stereomicroscope and analyzed offline. CT behavior was quantified with respect to change in body length over time as described in the cold plate assay.

Immunohistochemistry, confocal microscopy, and neuromorphometric analyses

Dissection, staining, mounting and confocal imaging of third instar larval filets were performed as previously described[66]. Primary antibodies: Rabbit anti-GFP (Molecular Probes, 1:500); Chicken anti-GFP (Aves Labs, 1:2000); Rabbit anti-Pkd2 (1:200, gift from Terry Watnick). Secondary antibodies were donkey anti-rabbit, donkey anti-chicken (1:300, Jackson Immunoresearch), goat-anti rabbit (1:250). IHC filets were imaged on a Nikon C1 Plus confocal microscope. For live confocal imaging, third instar larvae were immersed in a few drops of 1:5 (v/v) diethyl ether:halocarbon oil. Three

dimensional z-stacks were then volume rendered into a two-dimensional maximum projection and resultant images were processed for quantitative neuronal reconstruction analyses. Quantitative neuromorphometric analyses of dendritic arbors was performed as previously described[56].

Cell isolation and RT-PCR

Neuronal subpopulations were isolated using magnetic-bead-based cell sorting as previously described[67]. Following RNA purification from isolated cells (CIII or CIV da neurons), RT-PCR and data analyses were performed as previously described[66,67]**.** The following pre-validated Qiagen QuantiTect Primer Assays (Qiagen, Germantown, MD, USA) were used: *Pkd2* (QT00935347); *nompC* (QT00930139), and *Trpm* (QT00947261). Expression data were normalized using primers for RpL32 (QT00985677) and are reported as the mean fold change in expression ± s.d.

Microarray Expression Analyses

Microarray analyses of purified CIII da sensory neurons isolated from age-matched third instar larvae was performed as previously described[56]. Briefly, mRNA was isolated from independent pools of purified CIII da neurons (labeled by *ppk-Gal4,UAS-mCD8::GFP,ppk-Gal80*) via magnetic bead cell sorting (described above). mRNA isolation, amplification, labeling, and microarray hybridization were conducted by Miltenyi Biotec. 250 ng of CIII da neuron cDNAs were used as template for Cy3 labeling followed by hybridization to Agilent whole *Drosophila melanogaster* genome

oligo microarrays (4x44 K). For comparative analyses, these CIII da neuron microarray datasets were compared to our previously published CIV da neuron and whole larval microarray datasets (GSE46154[56]) which used an identical microarray chip allowing for direct comparisons. Statistical analyses of microarray data were performed as previously described[68]. Briefly, raw microarray data files obtained from the Agilent microarrays for CIII, CIV, and whole third instar larvae were read into GeneSpring GX software in which the data was quantile normalized and only those gene probes which are flagged positive and significantly expressed above background are selected for further analyses. Fold change in gene expression is calculated via the GeneSpring software and is based on mean expression values in cases where a given gene or isoform is represented by multiple probe IDs on the microarray. Fold changes for TRP channel gene expression were performed by comparing *class III_vs_whole larvae*; *class IV_vs_whole larvae*; and *class III_vs_class IV neurons*. Heat maps for the fold change values of these comparisons were constructed using *gplots* function in *R*. The fold change values are read into *R* and by using the *heatmap.2* function of *gplots* package, various heat maps of relative gene expression are constructed. The *heatmap.2* function allows for hierarchical clustering of genes based on their relative expression values. Fold-change values are scaled to z-scores for data visualization where red was selected to represent down-regulation (negative values) and green was selected to represent up-regulation (positive values). The z-score method scales the values of the fold change to -1 to +1 thereby facilitating visualization of changes in gene expression on the heat maps.

RESULTS

CIII da neurons mediate cold-evoked CT behavior

In order to examine the relative requirement of da neuron subtypes in mediating cold-evoked behavioral sensitivity, we electrically silenced da neurons individually via class-specific *GAL4*-mediated expression of a *UAS-tetanus toxin* transgene (*UAS-TNT-E*), subjected these transgenic larvae to global noxious cold stimulation at 6˚C and recorded cold-evoked behavioral responses. In these experiments, larval progeny expressing the *UAS-TNT-E* transgene via a specific *GAL4* driver were compared to wildtype *Oregon R* (*ORR*) and larvae bearing only the *UAS* or *GAL4* transgenes. Larvae expressing an inactive form of the tetanus toxin transgene (*UAS-IMP-TNT-V1A*) served as an additional negative control. In the cold plate assay, blockade of neural transmission in CIII da neurons (*CIII-GAL4*, *19-12-GAL4* or *nompC-GAL4*) most significantly attenuated CT behavior and increased NR behavior **(Fig.6)**. While *nompC-GAL4* labels CIII and chordotonal neurons, *19-12-GAL4* is specific for CIII. We also observed mild-to-moderate reductions in CT behavior and increased NR behavior upon silencing CI (*221-GAL4*) or CII (*GMR37B02-GAL4*) da neurons, however, silencing CIV (*477-GAL4;ppk1.9-GAL4*) da neurons had no effect on cold-evoked behaviors **(Fig.6)**. Simultaneous synaptic inhibition of CII and CIII da neurons with the *1003.3-GAL4* driver significantly inhibits the CT response and increased NR behavior, though not to the same extent that individual CIII specific drivers exhibit **(Fig.6)**. Interestingly, when CII and CIII da neurons are simultaneously silenced, a significant minority of these larvae exhibit

rolling behaviors in response to noxious cold; this is a unique observation as rolling behavior is normally elicited only in response to noxious heat or mechanical stimulation **(Fig.6)**. Together, these data support a dominant role for CIII da neurons, and a minor, perhaps modulatory role for CI and CII neurons, in mediating CT behavior to noxious cold stimuli in *Drosophila* larvae. The increase in other behaviors observed, such as rolling, may be due to a disinhibition of the circuitry required for those behaviors when CII and CIII neurons are silenced and fail to drive the CT circuitry.

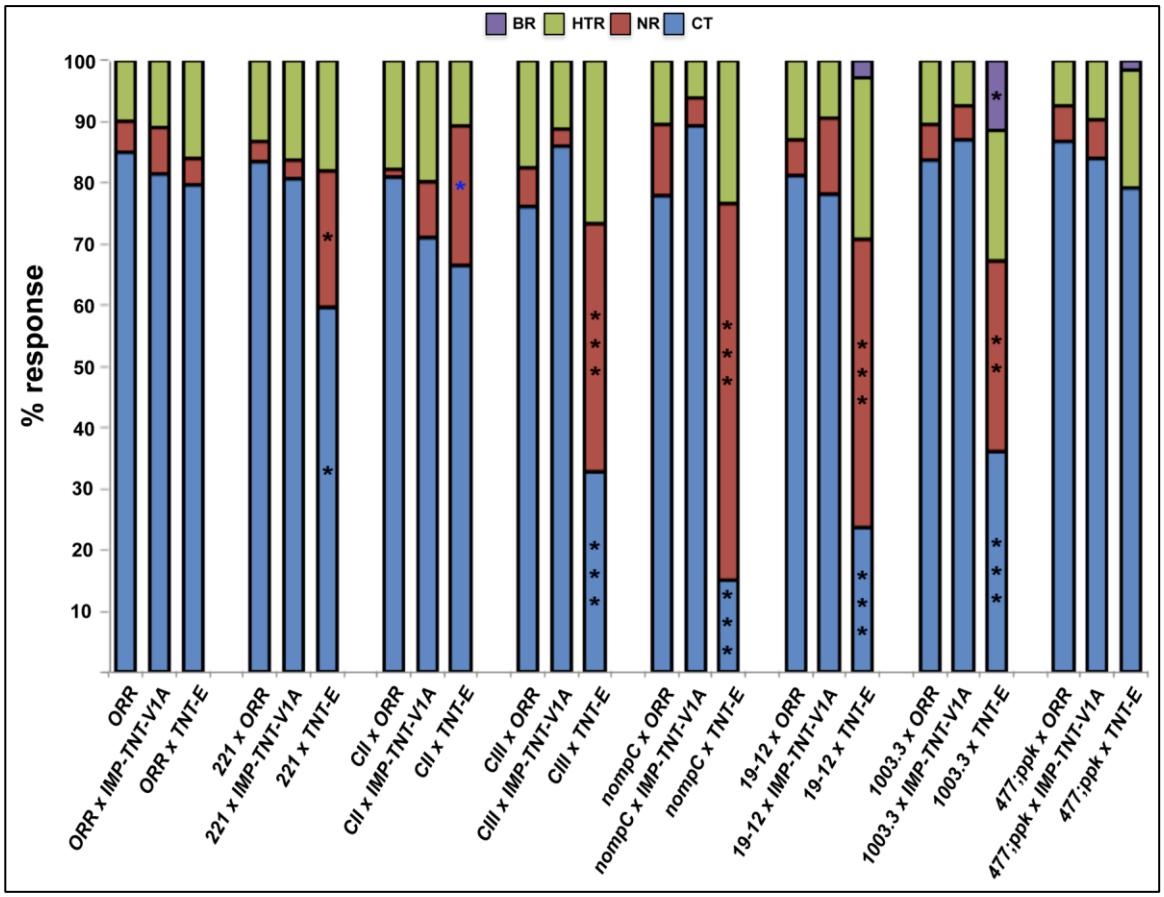

Figure 6. Percentage of Behaviors with class-specific inhibition of synaptic release. Fisher's exact test (two-tailed) with Bonferonni correction was used to assess differences in the percentages of behaviors individually with their appropriate controls. N=60-100 per genotype (* = p<.0125, ** = p<0.001, ***=p<0.0001). *CII* x *TNT-E* non-responders are labeled with (*) as three out of four comparisons had p<0.0125 (the Bonferonni correction significance threshold), but the comparison with *CII* x *IMP-TNT-V1A* was borderline significant at p<0.036. BR= body roll, NR= no response, HTR= head and/or tail raise, CT= contraction.

Optogenetic activation of CIII da neurons causes CT behavior

To examine whether direct activation of individual da neuron subtypes, in the absence of cold exposure, could elicit noxious cold-evoked behaviors, we expressed the ultrafast *UAS-channelrhodopsin-2* variant ChETA (*UAS-ChETA-YFP*)[55] via class-specific drivers. Control or experimental larvae bearing both the *GAL4* and *UAS* transgenes were stimulated with blue light in the presence or absence of all-*trans* retinal (ATR, a required co-factor for ChETA function) and the resulting behavioral responses were first evaluated qualitatively. Larvae lacking ATR in the food predominantly showed no change in their normal locomotive behavior when exposed to blue light; however, there was a small fraction of larvae which displayed HTR behavior under control conditions **(Fig.7)**. In contrast, larvae expressing the light-activated ChETA in CIII or CII da neurons, fed ATR, and exposed to blue light, produced a robust CT behavior within ≤1 second of light onset **(Fig.7)**. This response differed substantially from controls

(continued normal locomotion) as well as from the behavior observed in light touch assays[51,69,70]. Blue light activation of CI da neurons primarily resulted in a cessation of locomotion and a flaccid paralysis, whereas CIV activation produced the previously documented aversive rolling behavior[34] **(Fig.7)**. Quantitative analysis of larval change in length, similar to the cold plate assay, revealed CT and BR behaviors are easily distinguished from normal changes in body length during locomotion **(Fig.S1)**. Statistical comparison of CIII and CII optogenetically-induced CT behavior as a function of time reveals that CIII induced CT behavior is more sustained **(Fig.S2)** A significant portion of CII activated larvae (30%, data not shown) also displayed a HTR behavior after the initial CT behavior, which was not seen with CIII activated larvae. This suggests CII activation might partially be responsible for the HTR behavior. These data demonstrate that direct optogenetic activation of CIII, or CII, da neurons is sufficient to generate the cold-specific CT behavior, even in the absence of cold, and that CIII activation produces a more sustained CT response relative to CII neurons.

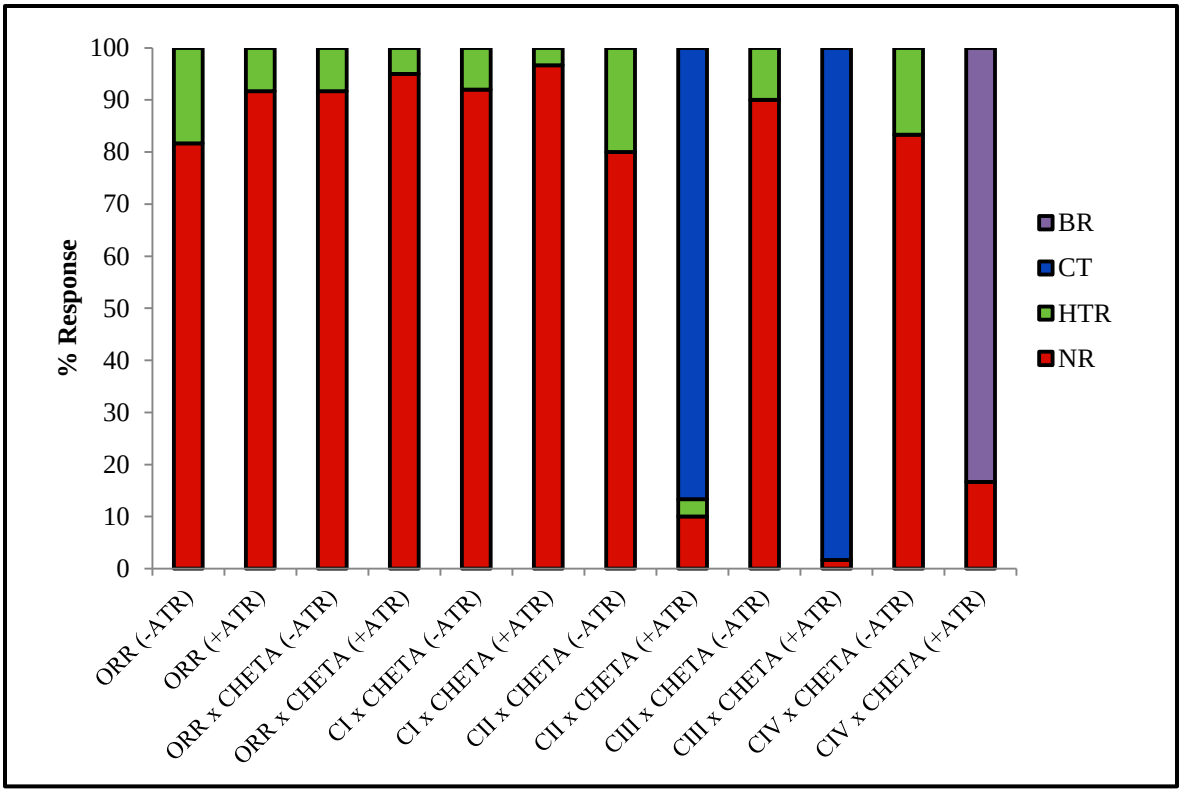

Figure 7. Optogenetic activation of CIII and CII neurons causes contracting behavior. Optogenetic activation of specific neurons was achieved by expressing a channelrhodopsin transgene (*UAS-ChETA-YFP)* with class specific drivers used previously. CIII and CII da neuron activation resulted in a phenocopy of the noxious cold induced CT behavior. Behaviors were qualitatively assessed. BR= body roll, NR= no response, HTR= head and/or tail raise, CT= contraction. N=20.

Simultaneous activation of CIII and CIV neurons results in CT behavior

In the larva, CIII and CIV da neuron dendrites tile on top of each other, such that their dendritic arbors are in very close proximity. Since optogenetic activation of CIII neurons results in a contraction behavior (CT), whereas activation of CIV neurons results

in a 360° aversive body roll behavior (BR), we wanted to determine what behavioral output could be observed upon directly stimulating both CIII and CIV neurons simultaneously. Specifically, we wanted to determine if, upon activation of both classes of neurons, one behavioral output was preferred or superseded the other. We found, upon simultaneous expression of *UAS-CHETA-YFP* in CIII and CIV neurons, that larvae produced a CT behavior in response to blue light activation **(Fig.8)**. This result suggests that at the circuit level, the CT behavioral response takes precedence over the aversive BR response when CIII and CIV neurons are simultaneously activated.

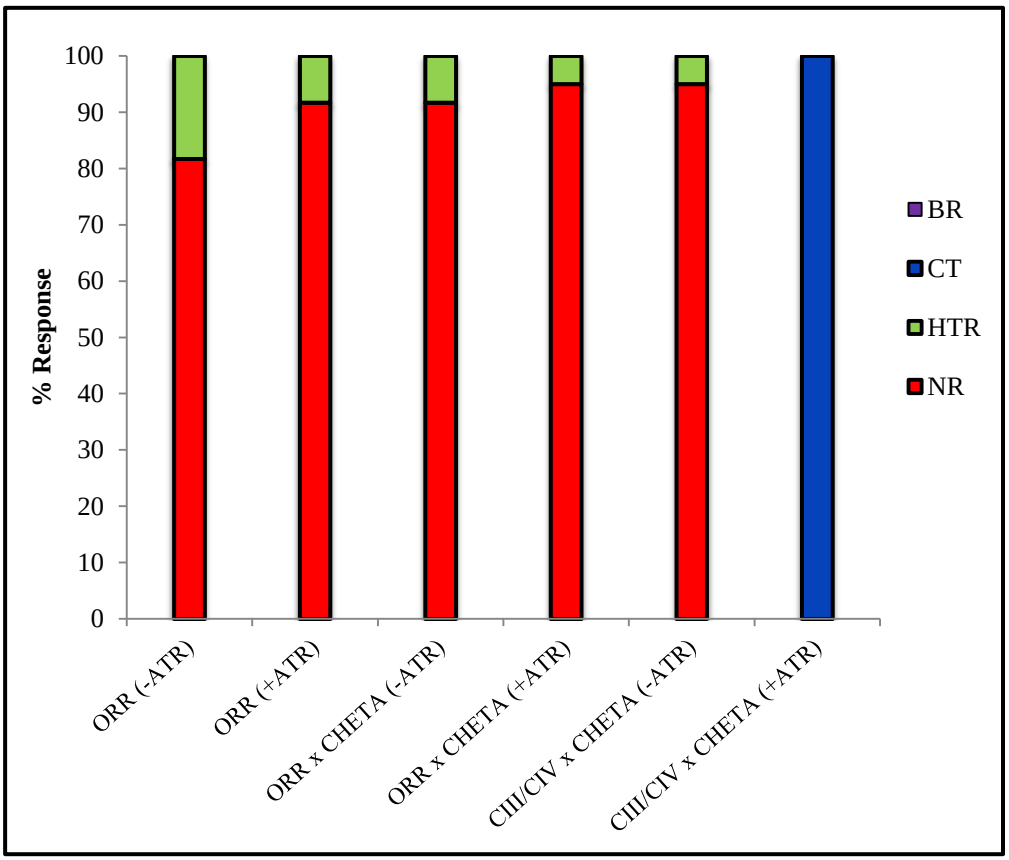

Figure 8. Simultaneous activation of CIII and CIV neurons results in CT behavior. Optogenetic activation of specific neurons was achieved by expressing a channelrhodopsin transgene (*UAS-ChETA-YFP)* with class specific drivers for CIII and CIV da neurons. CT behavior is dominant to BR behavior. Behaviors were qualitatively assessed. BR= body roll, NR= no response, HTR= head and/or tail raise, CT= contraction. N=15.

Cold stimulation results in specific Ca^{2+} responses within CIII da neurons

To investigate if da sensory neurons display Ca^{2+} responses to cold stimulation, we developed an *in vivo* preparation for live imaging of Ca^{2+} dynamics (see Experimental Procedures). Intact third instar larvae expressing GCaMP6 in da neurons through pan-md or class-specific drivers were live imaged to optically measure activation-induced Ca^{2+} responses to cold stimulation (6˚C). Relative to baseline fluorescence (F_0) at 25˚C, cold stimulation produced robust and sustained GCaMP6 signals with the greatest response occurring in CIII da neurons **(Fig. 9C)**. These findings are corroborated by statistical comparisons of average peak GCaMP6 signals in individual da neuron subtypes which demonstrate significantly higher peak fluorescence levels with cold stimulation in CIII neurons relative to other da neuron subclasses (CI, CII, & CIV) **(Fig. 9A,B,D,E)**. CII neurons also displayed significant increases in peak GCaMP6 signal with cold stimulation relative to CI and CIV da neurons, although this increase was not as large as that seen in CIII neurons **(Fig. 9E)**. To assess the specificity of cold-evoked GCaMP6 signals in da neuron subtypes as a function of temperature, we performed cross-

correlation analyses **(Fig. 9F)**. In these analyses, a negative cross-correlation coefficient indicates that maximal GCaMP6 signal occurred as the temperature declined. These analyses revealed a strong negative cross-correlation between GCaMP6 signal and temperature for CIII neurons. CIV da neurons also showed a strong negative correlation, though this was due to its relative silence at baseline coupled with a minimal increase in fluorescence at noxious cold temperatures. Moreover, CIII neurons show a minimal Ca^{2+} response to noxious heat stimulation (44ºC) **(Fig.S3)**, indicating their activity is specific to noxiously cold temperatures. Together, these results demonstrate that CIII, and to a lesser extent CII, neurons are noxious cold-activated.

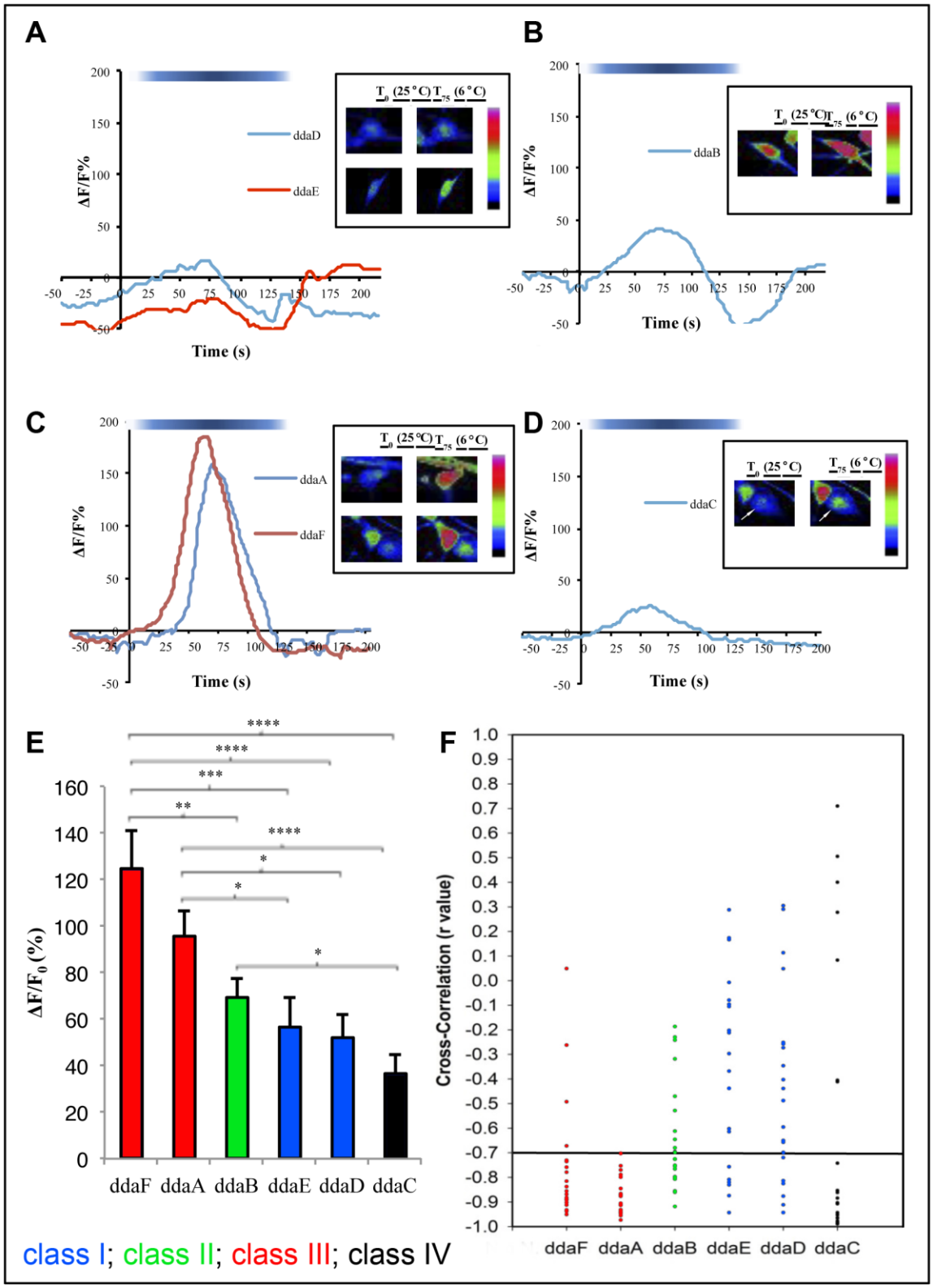
A
B
C
D
E
F
ddaD
ddaE
ddaB
ddaA
ddaF
ddaC
ΔF/F%
Time (s)
T0 (25 °C) T75 (6 °C)
ΔF/F0 (%)
Cross-Correlation (r value)
ddaF ddaA ddaB ddaE ddaD ddaC
class I; class II; class III; class IV

Figure 9. CIII sensory neurons are activated by cold. (A-D) Representative traces of $\Delta F/ F_0$ for da neurons: **(A)-** CI, **(B)-** CII, **(C)-** CIII, **(D)-** CIV. White-blue spectrum bar signifies temperature range (25°C-6°). Representative stills at 25°C and 6° are displayed next to each tracing. In Panel (**D**), the CIV ddaC neuron is marked by white arrows, whereas the adjacent cell with strong GCaMP6 response is a CIII ddaF neuron. **(E)** Data are expressed as average max $\Delta F/F_0$ + s.e.m. (F_0 being the average fluorescence signal 300 frames prior to stimulation temperature ramp). Statistical differences between each experimental group were assessed using a Mann-Whitney U Test. $p<0.05$= *, $p<0.01$=**, $p<0.001$=***, $p<0.0001$=**** (N=20 per da neuron). **(F)** Cross-correlation between temperature signal and raw fluorescence signal reveals that CIII Ca^{2+} responses are well correlated with decreases in temperature. The da neuron subtypes (CI-CIV) are color-coded for clarity in (**E,F**).

The TRP channels Pkd2, Trpm, and nompC are expressed in CIII da neurons

Comparative microarray analyses between CIII da neurons and whole third instar larval extracts were conducted to identify TRP channels that were significantly enriched in CIII neurons. In addition, we performed comparative expression analyses between CIII and CIV da neurons based on the observation that CIV neurons do not participate in noxious cold detection. Relative to whole larval homogenates, analyses of CIII expression data revealed significant enrichment of the TRP channels *nompC* and select *Trpm* isoforms **(Fig. 10A)**. Similarly, comparative analyses between CIII and CIV neurons revealed significant enrichment for *Pkd2* as well as *Trpm* RB and RC isoforms in

CIII neurons relative to CIV **(Fig. 10A)**. Interestingly, while *nompC* isoforms were enriched in CIII neurons compared to whole larvae, *nompC* isoform levels were not enriched in CIII relative to CIV neurons **(Fig. 10A)**. To confirm enriched expression of these TRP channels in CIII neurons, we independently isolated both CIII and CIV da neurons and performed comparative qRT-PCR. Both *nompC* and *Pkd2* were significantly enriched in CIII relative to CIV neurons, however, *Trpm* expression in CIII neurons showed only a mild increase, which was not significant **(Fig. 10B)**. This latter case could be due to the amplicon used in the qRT-PCR analyses recognizing multiple *Trpm* isoforms, possibly masking the overall expression levels. A number of other TRP channels (*trp, trpl, nan, wtrw, brv1, trpml*) were expressed in CIII da neurons, but were not enriched relative to whole larvae or CIV da neurons, whereas the TRPP molecule *brv2* was not detectable above background in CIII neurons (data not shown).

In addition to transcript expression, immunostaining of larval fillets with a Pkd2-specific antibody revealed protein expression on genetically-labeled CIII da neurons, including sensory filopodia **(Fig. 10C)**. *nompC* has previously been shown to be expressed in CIII neurons[23,24]; a promoter fragment from the *nompC* gene driving GAL4 expression labels CIII neurons[43] **(Fig. 10D)** and antibody labeling against nompC similarly labels these cells, including localization to sensory filopodia[23]. Collectively, these data suggest that these three TRP channels are present in the proper cells to play a role in cold-evoked behavior.

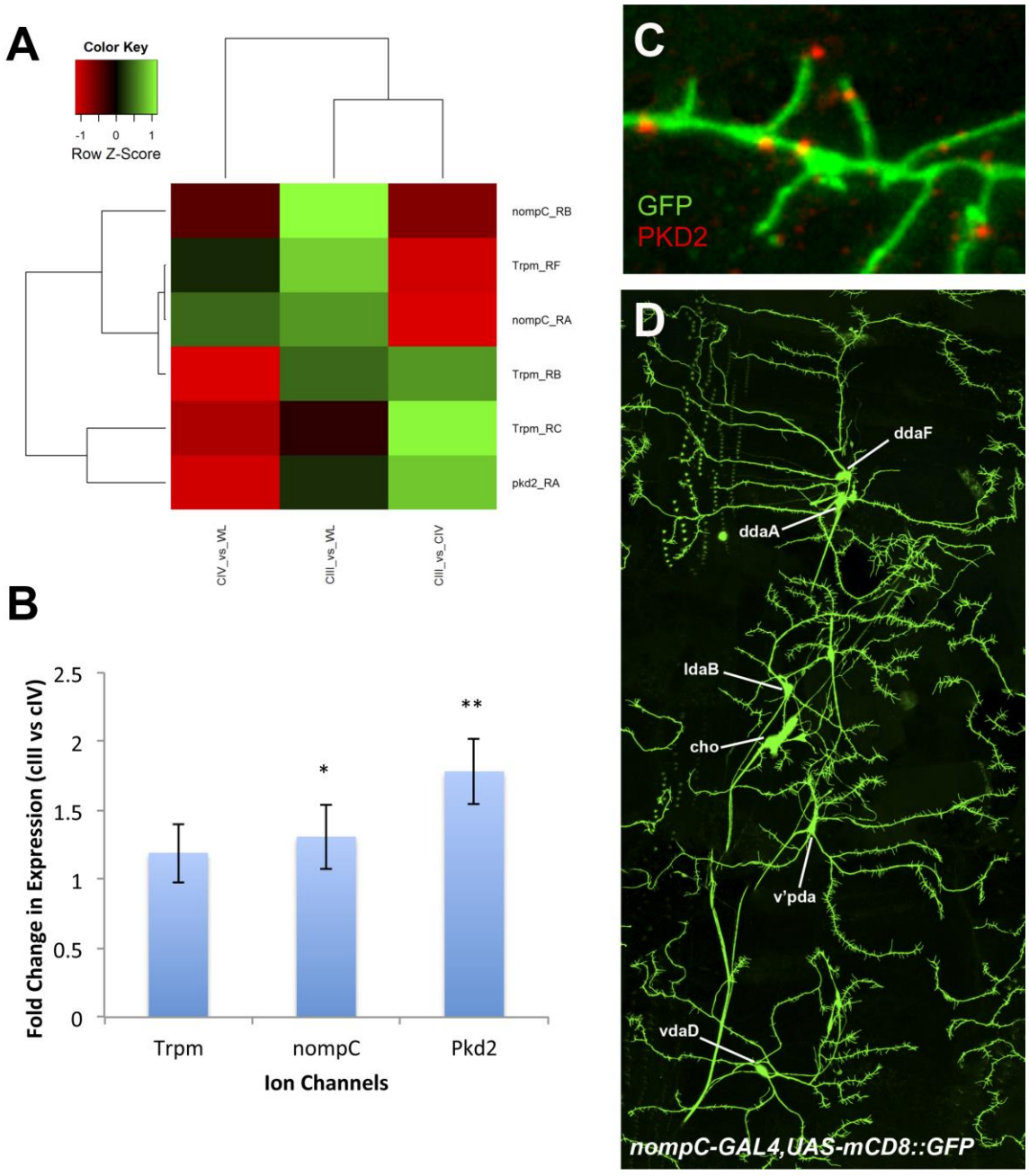

Figure 10. TRP channels *Pkd2*, *Trpm* and *nompC* are expressed in CIII sensory neurons. (A) Microarray analyses indicating enrichment of *Pkd2*, *Trpm*, and *nompC* isoforms in CIII vs CIV neurons and comparing expression between CIII and whole larva and CIV and whole larva. The color key represents z-score enrichment, green being more

enriched and red indicating not enriched or not present. **(B)** qRT-PCR analysis of *Pkd2*, *Trpm*, and *nompC* expression in CIII vs. CIV. Mann-Whitney U-Test, *=p<0.05, **=p<0.01 (N=4). **(C)** Pkd2 antibody staining (red) corresponds with CIII neurons marked (green). **(D)** *nompC-GAL4* driven expression of *UAS-mCD8::GFP* corresponds to CIII neuron expression.

Pkd2, Trpm, nompC function in CIII da neurons in noxious cold detection

To test whether these TRP channels enriched in CIII da neurons are required for noxious cold detection, we first asked whether viable whole animal mutants for these genes exhibit normal behavioral responses to noxious cold stimuli. Homozygous null mutant larvae of *Pkd2*, *nompC,* or *Trpm* displayed significantly reduced cold-evoked CT responses and increased HTR responses **(Fig.11A)**. A significant number of *Pkd2* and *Trpm* mutants also exhibited increased NR as well as BR behaviors; BR behavior is not normally observed in control conditions, but rather in response to noxious heat and mechanical stimulation **(Fig.11A)**. Only one whole mutant *nompC* larvae exhibited BR. Transheterozygous combinations of the *Pkd2* and *Trpm* null mutant allele and their corresponding deficiency also significantly impaired the CT response and increased the HTR response, similar to the homozygous null mutant larvae results **(Fig.11A)**. NR was only increased in the transheterzygous combinations involving *Pkd2,* not *Trpm*. The BR response in transheterozygous combinations of *Pkd2* and *Trpm* were reduced when compared to homozygous null mutants. A transheterozygous combination of the *nompC*

null mutant allele and corresponding deficiency did not impair CT, HTR, NR or BR response **(Fig.11A)**.

To test whether these genes function in CIII da neurons, as predicted by their expression, we expressed gene-specific *UAS-RNAi* transgenes targeting each TRP channel of interest. Larvae expressing RNAi transgenes targeting *Pkd2, Trpm* and *nompC* in CIII neurons showed significant decreases in CT behavior and increased NR behavior compared to control larvae **(Fig.11C)**. An increase in HTR response was only found in one *nompC-RNAi* line. BR was seen at non-significant levels in two of the *Pkd2-RNAi* lines and one of the *Trpm-RNAi* lines.

In addition to demonstrating CIII gene functioning with RNAi, we were able to rescue cold-evoked CT and BR behavior in *Pkd2* mutants by reintroducing *Pkd2* into CIII neurons using UAS transgenes **(Fig.11B)**. Homozygous null larvae with just the *UAS-Pkd2* transgene, and no GAL4, also demonstrated a rescue of CT and BR behavior **(Fig.11B)**. This may be due to leaky background expression of *UAS-Pkd2* in the absence of GAL4 since larvae with wildtype *Pkd2* and just *UAS-Pkd2* did not reveal any deficits. Interestingly, reintroducing *nompC* into CIII neurons with a *UAS-nompC-GFP* transgene on one or both chromosomes did not reduce the increased HTR response we saw in homozygous null mutants **(Fig.11B)**.

To assess the putative role of these TRP channels in mediating cold-evoked CT behavior, we performed functional optogenetic assays in which we simultaneously expressed *UAS-ChETA-YFP* and RNAi transgenes for *Pkd2, nompC* or *Trpm* in CIII neurons in order to examine whether these channels function in the transduction or

propagation of noxious cold stimuli. Consistent with known roles for TRP channels, disruption of *nompC, Pkd2* or *Trpm* in CIII neurons failed to attenuate optogenetically-induced CT behavior suggesting these channels operate in the sensory transduction phase, rather than the propagation phase (**Fig.S4**). Moreover, we find that disruption of *Pkd2, Trpm* or *nompC* function in CIII neurons, via TRP-specific RNAi transgenes, had no significant effect on CIII dendritic morphology (**Fig.S5)**.

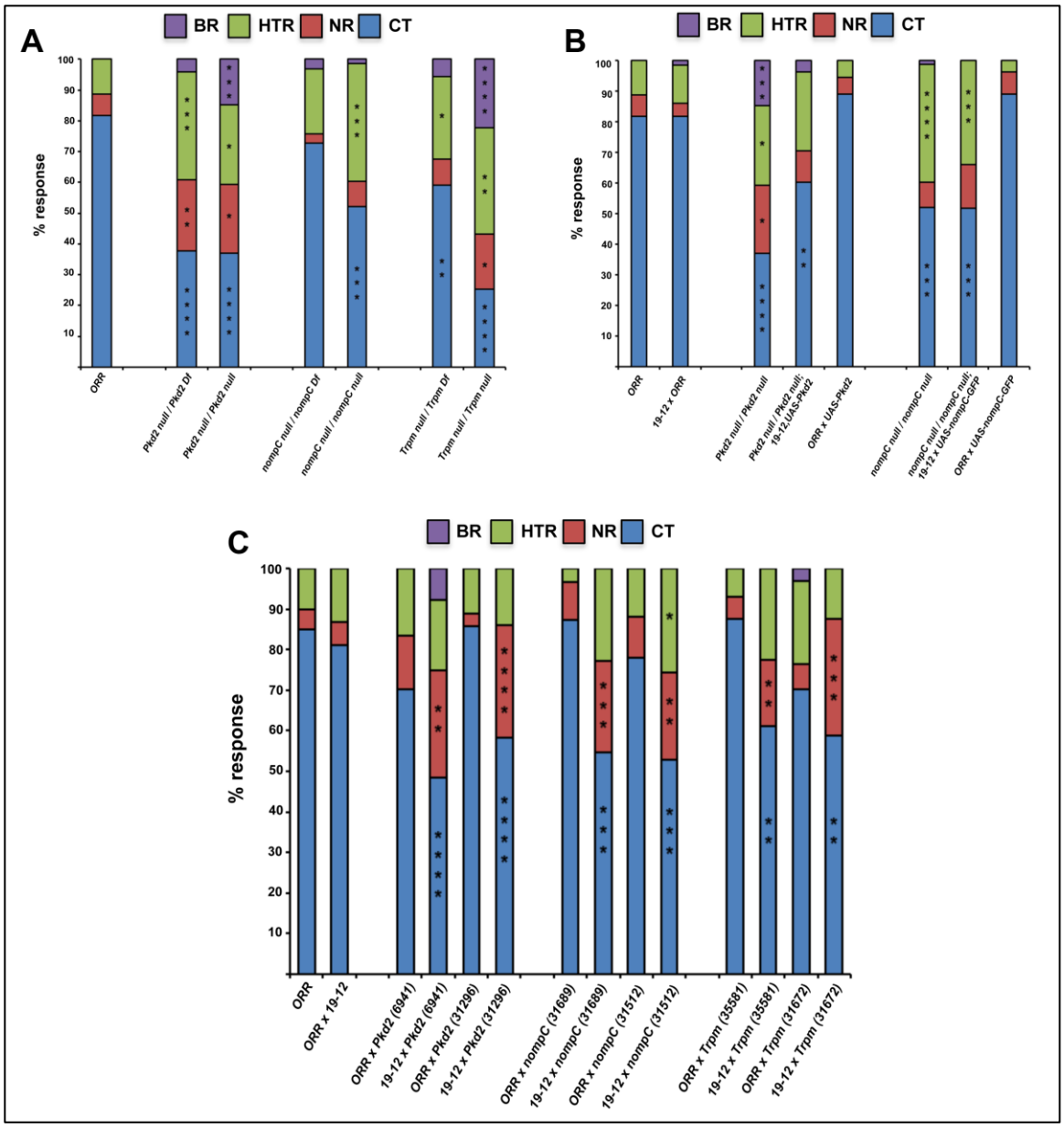

Figure 11. Pkd2, Trpm and nompC mediate normal CT behavior in CIII da neurons.

(A) *Pkd2* mutants and *Trpm* mutants exhibit altered levels of NR, HTR, CT, and BR. nompC mutants exhibit altered levels of HTR and CT. Transheterzygous combinations of null alleles and corresponding deficiencies exhibit slightly different patterns: *Pkd2*- altered NR, HTR, and CT; *Trpm*- altered HTR and CT; *nompC*- not significantly

different from control behaviors. **(B)** Expression of *UAS-Pkd2* in CIII da neurons rescues CT and eliminates significant BR and NR behavior in whole mutant backgrounds. In contrast, expression of *UAS-nompC-GFP* alone in CIII neurons of a *nompC* null mutant background is insufficient to significantly rescue CT behavior. Overexpression of *UAS-Pkd2* or *UAS-nompC-GFP* in CIII neurons does not significant disrupt any observed behavior relative to controls. **(C)** *Pkd2*, *Trpm*, and *nompC* RNAi knockdown predominantly alters larval levels of CT and NR behaviors (confirmed in (2) independent gene-specific RNAi lines). Fisher's exact test (two-tailed) with Bonferonni correction was used to assess differences in the percentages of behaviors individually with their appropriate controls. *=$p<0.05$, **=$p<0.01$, ***=$p<0.001$ ****=$p<0.0001$. N=60-81.

DISCUSSION

Here we have established a novel behavioral assay for acute cold nociception in *Drosophila* larvae. The primary cold-evoked behavior, contraction (CT), is unlike larval responses to other types of innocuous and nociceptive stimuli[14,20,22–24,37,44]. Several lines of evidence support the role of CIII neurons as cold nociceptors. First, synaptically silencing CIII da neurons dramatically impairs the CT response, with numerous larvae displaying NR. Second, direct optogenetic activation of CIII da neurons results in a phenocopy of the normal CT behavior in response to noxious cold stimulation. CII optogenetic activation also results in CT behavior; however, CIII optogenetically-induced CT is followed by a longer period of immobilization, which is more similar to native exposure of noxious cold stimuli. Third, CIII da neurons exhibit large somal Ca^{2+} fluctuations in response to noxious cold stimuli, but not in response to the baseline temperature of 25ºC or noxious heat temperature of 44º C.

Given that CIII neurons also mediate behavioral responses to gentle touch[23,24], their requirement for cold nociception makes them, like CIV neurons, multimodal. In vertebrates, multimodal sensory afferents have been documented as well, e.g., mechanosensitive afferent fibers that respond to noxious heat/cold[71]. It remains, though, an open question how multimodal neurons differentiate between the numerous distinct stimuli and how their signal initiates the correct downstream behavioral response. This will be a particularly challenging question for the CIII neurons moving forward as light touch and cold evoked distinct behaviors appear to require the nompC TRP channel. One

possible explanation for the different behavioral outputs is that the different input stimuli engage different suites of channels, with each making a distinct contribution to the downstream signal. Other neurons, with different sensitivities, may also be contributing in subtle ways to the neural signals the final behavioral decision is based upon.

At the molecular level, Pkd2, nompC, and Trpm, are enriched in CIII neurons and function in these cells to mediate the contraction response to noxious cold. Interestingly, nompC also plays a role in CIII neurons in the gentle touch response[23,24]; however, as proposed above, gentle touch utilizes a set of channels that includes nompC, ripped pocket and NMDAR[51], whereas cold engages, Pkd2, and Trpm in addition to nompC. nompC is not the only TRP channel in *Drosophila* that has multiple functions. *painless* is required for both noxious mechanical, high heat sensing in larvae[20] as well as thermal sensitization[13]. Similarly, dTRPA1 responds to high temperatures[27,46], and is required for thermal preference[35,47–49], chemical nociception[50,51], thermal hyperalgesia[13], and responses to high-intensity light[45]. For *painless* and *dTRPA1* this multimodality may be regulated by specific splice variants mediating distinct functions, however other mechanisms are possible.

Furthermore Pkd2, like nompC, is broadly multimodal in sensory transduction. In addition to its role in cold, Pkd2 has also been implicated in taste sensing in vertebrates[52,53]. Pkd2 is also required for mechanosensitive calcium currents in the primary cilia of the kidney epithelium[54]. This function may be related to its role as a causative gene in autosomal dominant polycystic kidney disease, a common life threatening disorder. Currently, it is unclear if patients suffering from this disease, or in

mouse models lacking the gene[55], result in defects in thermal nociception. Lastly, although TRPM8 acts a cold sensor in vertebrates[7,31,56], ours is the first evidence that a Trpm family member acts as a cold sensor in *Drosophila.*

At the circuit level, it is, as yet, unclear why certain manipulations resulted in an increase in HTR and rolling behavior at 6ºC. For instance, at 6ºC, simultaneous synaptic inhibition of CII and CIII da neurons results in a minority of larvae exhibiting rolling behavior; the presence of rolling behavior is unusual as this behavioral response is normally only elicited in response to noxious heat and mechanosensation. We also observed, at 6ºC, increased HTR in *Pkd2, nompC,* and *Trpm* whole mutants, and rolling behavior in *Pkd2* and *Trpm* mutants. These other behaviors are likely being activated as a compensatory aversive escape behavior. Given that all da neurons show at least a small Ca^{2+} fluctuation in response to noxious cold stimulation, it is plausible that in the absence of sufficient CIII signaling, signals from other sensory neurons may exert more influence on downstream circuits, ultimately resulting in a different behavioral output. In fact, given recent findings demonstrating the compensatory nature of hot and cold sensing circuitry[19], it is likely larvae with impaired noxious cold detection are hypersensitive to heat detection and rolling in response to cold may be evidence of that.

Taken together, our results identify the peripheral sensory neurons responsible for noxious cold detection in *Drosophila* larvae and the conserved molecular players required for this process. Our novel cold assays offer a powerful new model for the genetic dissection of cold nociception. Further exploitation of this model should yield exciting insight into cold nociception to probe as yet unanswered questions about this

understudied sensory modality and the neural circuitry that drives nociceptive behavior. Moreover, given the distinct roles of CIII and CIV neurons in noxious cold and noxious heat nociception, respectively, this system provides an excellent platform for investigating the circuit basis for labeled lines that modulate distinct behavioral output to a range of sensory stimuli.

SUPPLEMENTAL FIGURES

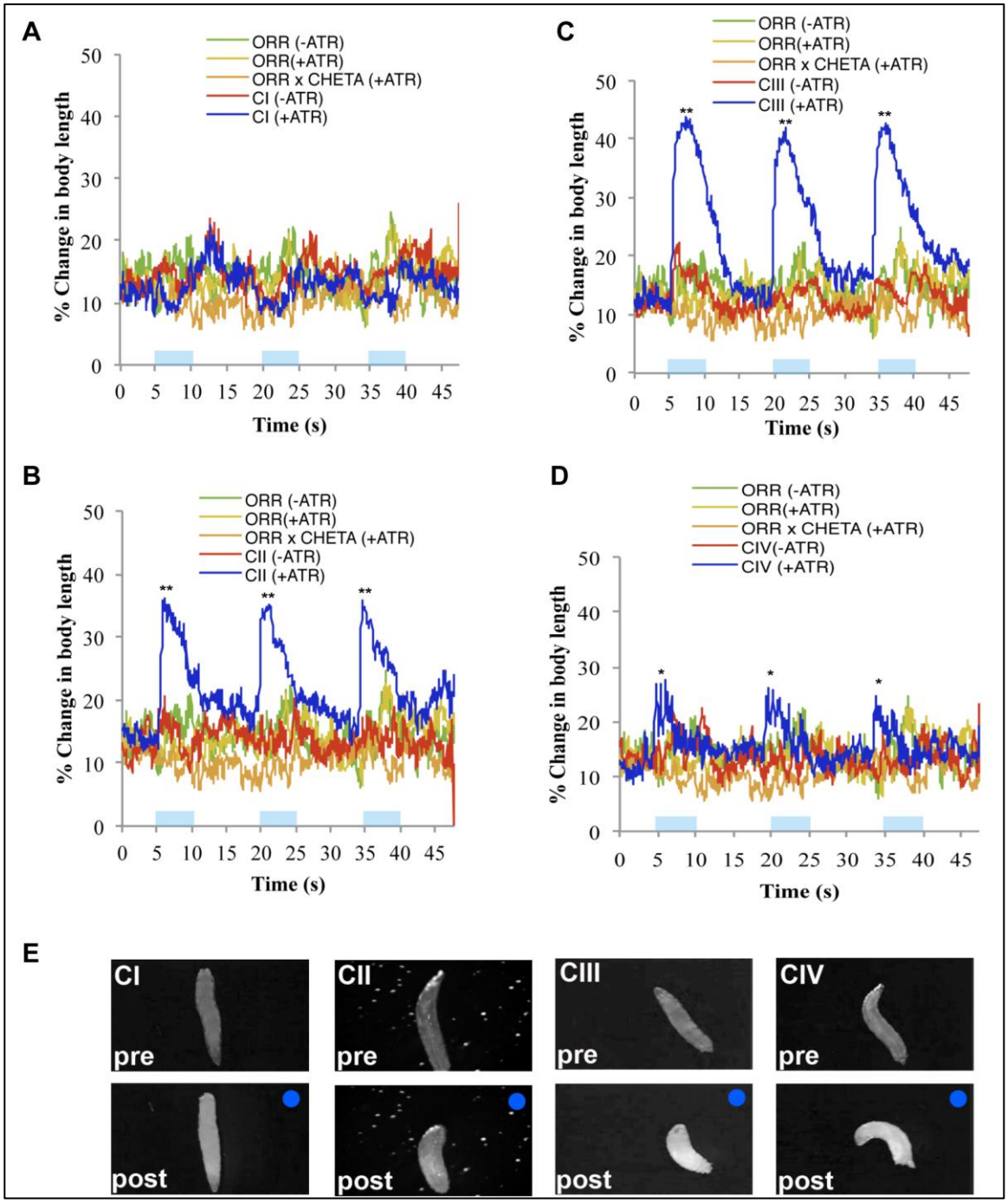

Figure S1. Quantitative analyses of optogenetic induced behavior in da neurons. **(A)** Optogenetic activation of CI da neurons fails to significantly change larval length. **(B)** Optogenetic activation of CII da neurons results in a significant change in larval length consistent with CT. **(C)** Optogenetic activation of CIII da neurons result in a significant change in larval length consistent with CT. **(D)** Optogenetic activation of CIV da neurons results in a significant change in larval length consistent with BR. Shaded blue boxes (**A-D**) indicate duration of the 480nm light stimulation. A two-tailed t-test was used to calculate significance. N=15-20. *=$p<0.01$, **=$p<<0.01$. (**E**) Pre- and post-optogenetic stimulation images of third instar larval behaviors with CI, CII, CIII, or CIV specific activation.

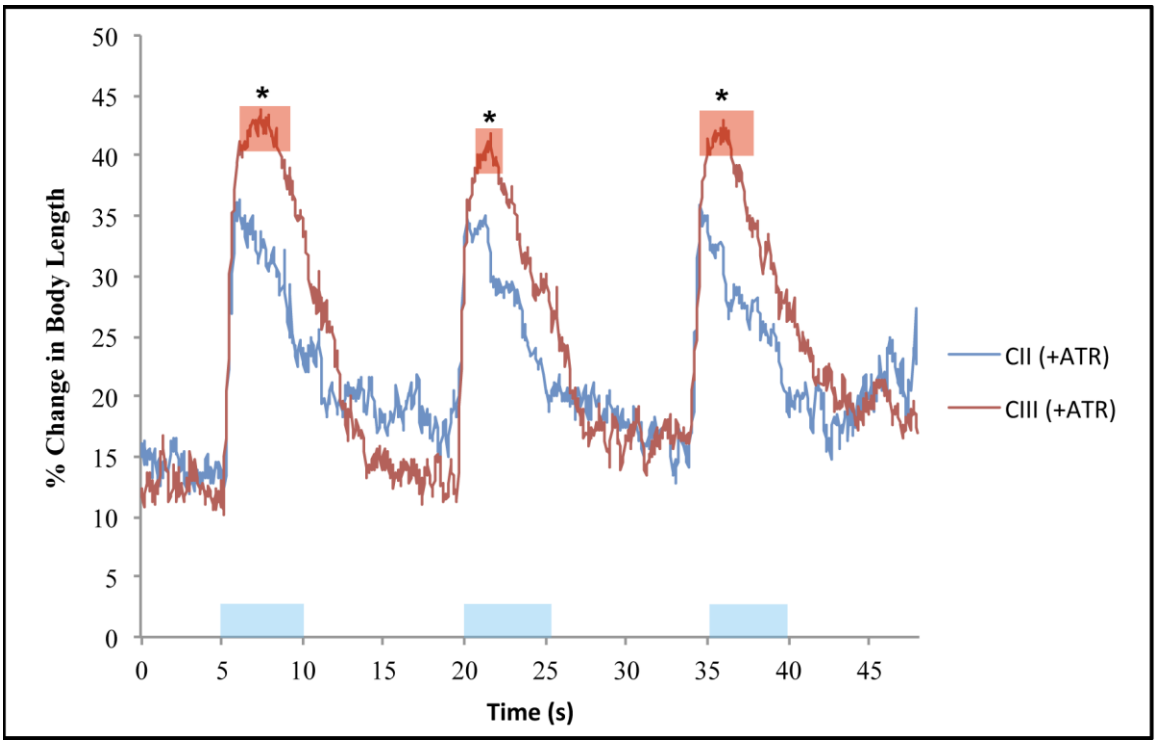

Figure S2. CIII-induced CT is more sustained than CII-induced CT. Shaded red boxes indicate time period in which larvae exhibit significantly increased change in body length. Light blue box indicates duration of 480nm light stimulation. Significance was assessed with a two-tailed t-test. N=20. *=$p<0.05$.

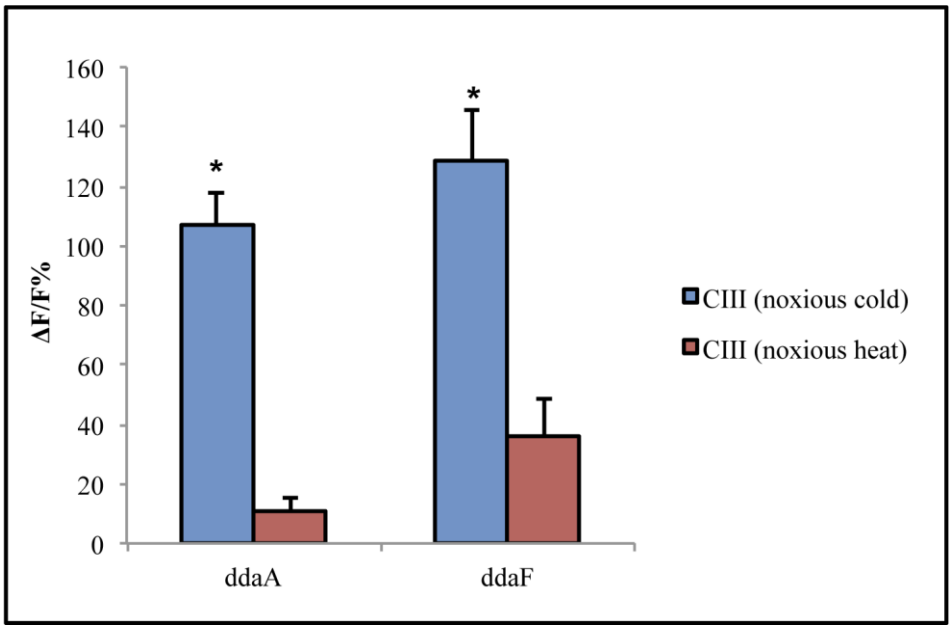

Figure S3. CIII da neurons respond minimally to noxious heat. A two-tailed Mann-Whitney U test was used to assess differences in max CIII $\Delta F/F_0$ under noxious cold and heat exposure. N=10. *=$p<0.001$

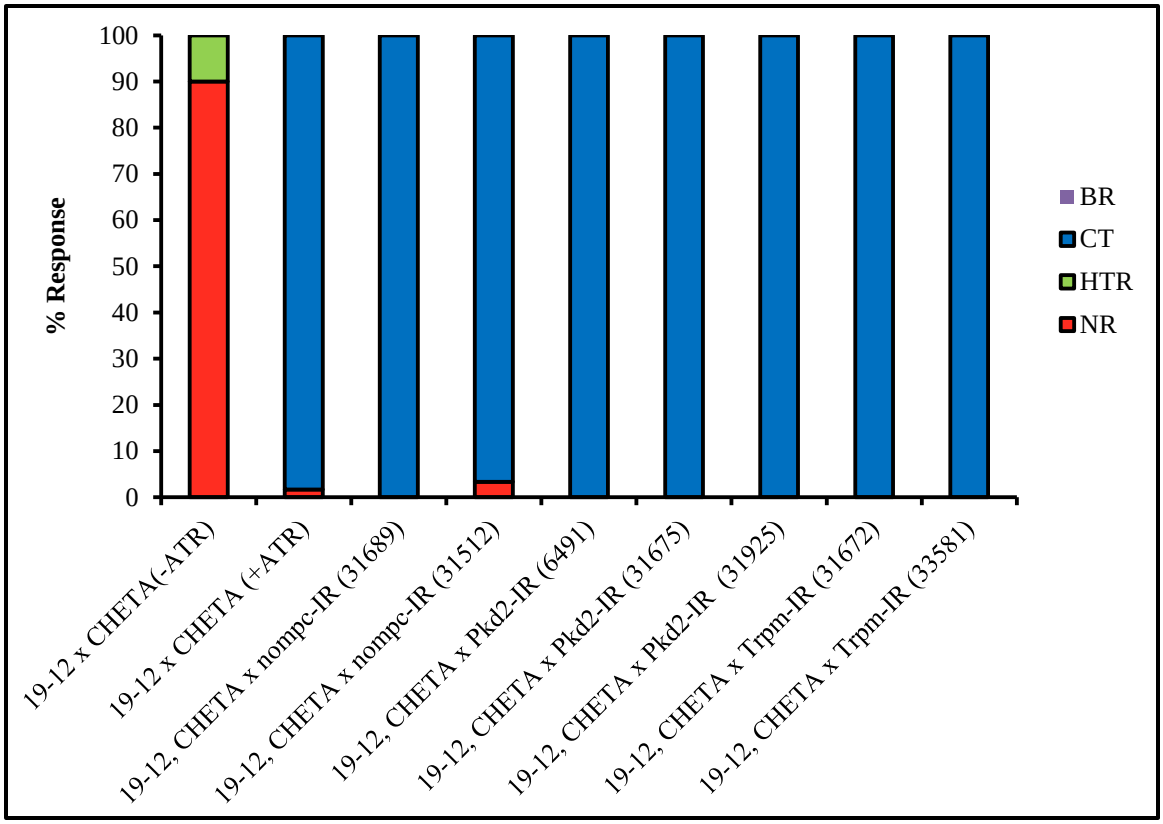

Figure S4. Functional optogenetics reveal TRP channels function at transduction stage. The presence of an intact CT response indicates that action potential propagation in CIIIs is left intact with TRP channel knockdown. This supports the role of these select TRP channels at the transduction stage. BR= body roll; CT= contraction; HTR= head and/or tail raise; NR= no response. N=20.

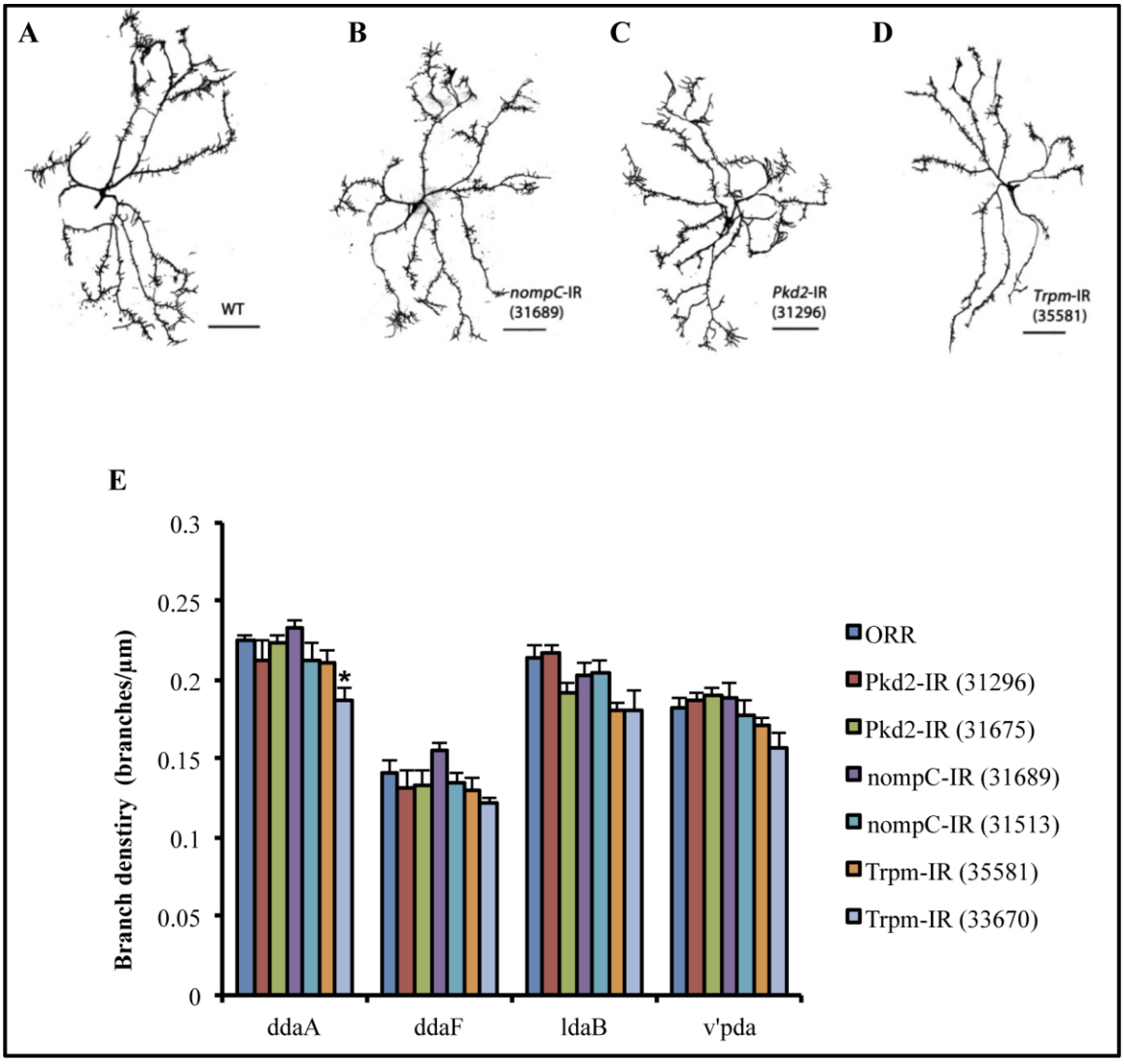

Figure S5. TRP channel knockdown does not affect CIII morphology. (A-D) Representative CIII (v'pda) images. **(E)** Average branch density measured in branches/µm. A two-tailed t-test and Bonferonni correction were used. N=8-10. *=p<0.008

LIST OF REFERENCES

1. Bromm, B. & Treede, D.-R. Withdrawal reflex, skin resistance reaction and pain ratings due to electrical stimuli in man: *Pain* **9,** 339–354 (1980).

2. Le Bars, D., Gozariu, M. & Cadden, S. W. Animal models of nociception. *Pharmacol. Rev.* **53,** 597–652 (2001).

3. Ewan St John Smith, G. R. L. Nociceptors: a phylogenetic view. *J. Comp. Physiol. A Neuroethol. Sens. Neural. Behav. Physiol.* **195,** 1089–106 (2009).

4. Sneddon, L. U. Evolution of nociception in vertebrates: comparative analysis of lower vertebrates. *Brain Res. Brain Res. Rev.* **46,** 123–130 (2004).

5. Tobin, D. M. & Bargmann, C. I. Invertebrate nociception: Behaviors, neurons and molecules. *J. Neurobiol.* **61,** 161–174 (2004).

6. Basbaum, A. I., Bautista, D. M., Scherrer, G. & Julius, D. Cellular and molecular mechanisms of pain. *Cell* **139,** 267–284 (2009).

7. Lumpkin, E. A. & Caterina, M. J. Mechanisms of sensory transduction in the skin. *Nature* **445,** 858–865 (2007).

8. Woolf, C. J. & Ma, Q. Nociceptors—Noxious Stimulus Detectors. *Neuron* **55,** 353–364 (2007).

9. Tracey, I. & Mantyh, P. W. The cerebral signature for pain perception and its modulation. *Neuron* **55,** 377–391 (2007).

10. Bostock, H., Campero, M., Serra, J. & Ochoa, J. L. Temperature-dependent double spikes in C-nociceptors of neuropathic pain patients. *Brain J. Neurol.* **128,** 2154–2163 (2005).

11. Becerra, L. *et al.* Trigeminal neuropathic pain alters responses in CNS circuits to mechanical (brush) and thermal (cold and heat) stimuli. *J. Neurosci. Off. J. Soc. Neurosci.* **26,** 10646–10657 (2006).

12. Baron, R. Mechanisms of Disease: neuropathic pain—a clinical perspective. *Nat. Clin. Pract. Neurol.* **2,** 95–106 (2006).

13. Costigan, M., Scholz, J. & Woolf, C. J. Neuropathic pain: a maladaptive response of the nervous system to damage. *Annu. Rev. Neurosci.* **32,** 1–32 (2009).

14. Bruce Nicholson, M. D. Differential Diagnosis: Nociceptive and Neuropathic Pain. *Am. J. Manag. Care* **12,** (2006).

15. Van Laar, M. *et al.* Pain treatment in arthritis-related pain: beyond NSAIDs. *Open Rheumatol. J.* **6,** 320–330 (2012).

16. Greg, D., erson & MD. Understanding Neuropathic Pain. *SpineUniverse* at <http://www.spineuniverse.com/conditions/chronic-pain/understanding-neuropathic-pain>

17. Schepers, R. J. & Ringkamp, M. Thermoreceptors and thermosensitive afferents. *Neurosci. Biobehav. Rev.* **33,** 205–212 (2009).

18. Szallasi, A., Cortright, D. N., Blum, C. A. & Eid, S. R. The vanilloid receptor TRPV1: 10 years from channel cloning to antagonist proof-of-concept. *Nat. Rev. Drug Discov.* **6,** 357–372 (2007).

19. McCoy, E. S. *et al.* Peptidergic CGRPα Primary Sensory Neurons Encode Heat and Itch and Tonically Suppress Sensitivity to Cold. *Neuron* **78,** 138–151 (2013).

20. Brandt, M. R., Beyer, C. E. & Stahl, S. M. TRPV1 Antagonists and Chronic Pain: Beyond Thermal Perception. *Pharmaceuticals* **5,** 114–132 (2012).

21. Babcock, D. T., Landry, C. & Galko, M. J. Cytokine Signaling Mediates UV-Induced Nociceptive Sensitization in Drosophila Larvae. *Curr. Biol.* **19,** 799–806 (2009).

22. Babcock, D. T. *et al.* Hedgehog signaling regulates nociceptive sensitization. *Curr. Biol. CB* **21,** 1525–1533 (2011).

23. Kim, S. E., Coste, B., Chadha, A., Cook, B. & Patapoutian, A. The role of Drosophila Piezo in mechanical nociception. *Nature* **483,** 209–212 (2012).

24. Neely, G. G. *et al.* Construction of a global pain systems network highlights phospholipid signaling as a regulator of heat nociception. *PLoS Genet.* **8,** e1003071 (2012).

25. Im, S. H. & Galko, M. J. Pokes, sunburn, and hot sauce: Drosophila as an emerging model for the biology of nociception. *Dev. Dyn. Off. Publ. Am. Assoc. Anat.* **241,** 16–26 (2012).

26. Caldwell, J. C. & Tracey, W. D. Alternatives to mammalian pain models 2: using Drosophila to identify novel genes involved in nociception. *Methods Mol. Biol. Clifton NJ* **617,** 19–29 (2010).

27. Manev, H. & Dimitrijevic, N. Drosophila model for in vivo pharmacological analgesia research. *Eur. J. Pharmacol.* **491,** 207–208 (2004).

28. Liu, L., Yermolaieva, O., Johnson, W. A., Abboud, F. M. & Welsh, M. J. Identification and function of thermosensory neurons in Drosophila larvae. *Nat. Neurosci.* **6,** 267–273 (2003).

29. Gallio, M., Ofstad, T. A., Macpherson, L. J., Wang, J. W. & Zuker, C. S. The coding of temperature in the Drosophila brain. *Cell* **144,** 614–624 (2011).

30. Neely, G. G. *et al.* A genome-wide Drosophila screen for heat nociception identifies α2δ3 as an evolutionarily conserved pain gene. *Cell* **143,** 628–638 (2010).

31. Bodmer, R. & Jan, Y. N. Morphological differentiation of the embryonic peripheral neurons in Drosophila. *Rouxs Arch. Dev. Biol.* **196,** 69–77 (1987).

32. Brewster, R. & Bodmer, R. Origin and specification of type II sensory neurons in Drosophila. *Dev. Camb. Engl.* **121,** 2923–2936 (1995).

33. Tracey, W. D., Wilson, R. I., Laurent, G. & Benzer, S. painless, a Drosophila gene essential for nociception. *Cell* **113,** 261–273 (2003).

34. Hwang, R. Y. *et al.* Nociceptive neurons protect Drosophila larvae from parasitoid wasps. *Curr. Biol. CB* **17,** 2105–2116 (2007).

35. Zhong, L., Hwang, R. Y. & Tracey, W. D. Pickpocket is a DEG/ENaC protein required for mechanical nociception in Drosophila larvae. *Curr. Biol. CB* **20,** 429–434 (2010).

36. Grueber, W. B., Jan, L. Y. & Jan, Y. N. Tiling of the Drosophila epidermis by multidendritic sensory neurons. *Dev. Camb. Engl.* **129,** 2867–2878 (2002).

37. Nilius, B. & Owsianik, G. The transient receptor potential family of ion channels. *Genome Biol.* **12,** 218 (2011).

38. Venkatachalam, K. & Montell, C. TRP Channels. *Annu. Rev. Biochem.* **76,** 387–417 (2007).

39. Montell, C. *et al.* A Unified Nomenclature for the Superfamily of TRP Cation Channels. *Mol. Cell* **9,** 229–231 (2002).

40. Caterina, M. J. *et al.* The capsaicin receptor: a heat-activated ion channel in the pain pathway. *Nature* **389,** 816–824 (1997).

41. Peier, A. M. *et al.* A TRP Channel that Senses Cold Stimuli and Menthol. *Cell* **108,** 705–715 (2002).

42. Sarria, I., Ling, J., Xu, G.-Y. & Gu, J. G. Sensory discrimination between innocuous and noxious cold by TRPM8-expressing DRG neurons of rats. *Mol. Pain* **8,** 79 (2012).

43. Story, G. M. *et al.* ANKTM1, a TRP-like channel expressed in nociceptive neurons, is activated by cold temperatures. *Cell* **112,** 819–829 (2003).

44. Babes, A., Zorzon, D. & Reid, G. A novel type of cold-sensitive neuron in rat dorsal root ganglia with rapid adaptation to cooling stimuli. *Eur. J. Neurosci.* **24,** 691–698 (2006).

45. Munns, C., AlQatari, M. & Koltzenburg, M. Many cold sensitive peripheral neurons of the mouse do not express TRPM8 or TRPA1. *Cell Calcium* **41,** 331–342 (2007).

46. Bautista, D. M. *et al.* The menthol receptor TRPM8 is the principal detector of environmental cold. *Nature* **448,** (2007).

47. Rosenzweig, M., Kang, K. & Garrity, P. A. Distinct TRP Channels Are Required for Warm and Cool Avoidance in Drosophila melanogaster. *Proc. Natl. Acad. Sci. U. S. A.* **105,** 14668–14673 (2008).

48. Fowler, M. A. & Montell, C. Drosophila TRP channels and animal behavior. *Life Sci.* **92,** 394–403 (2013).

49. Duffy, J. B. GAL4 system in drosophila: A fly geneticist's swiss army knife. *genesis* **34,** 1–15 (2002).

50. Southall, T. D., Elliott, D. A. & Brand, A. H. The GAL4 System: A Versatile Toolkit for Gene Expression in Drosophila. *CSH Protoc.* **2008,** pdb.top49 (2008).

51. Tsubouchi, A., Caldwell, J. C. & Tracey, W. D. Dendritic Filopodia, Ripped Pocket, NOMPC, and NMDARs Contribute to the Sense of Touch in Drosophila Larvae. *Curr. Biol.* **22,** 2124–2134 (2012).

52. Watnick, T. J., Jin, Y., Matunis, E., Kernan, M. J. & Montell, C. A flagellar polycystin-2 homolog required for male fertility in Drosophila. *Curr. Biol. CB* **13,** 2179–2184 (2003).

53. Jenett, A. *et al.* A GAL4-driver line resource for Drosophila neurobiology. *Cell Rep.* **2,** 991–1001 (2012).

54. Xiang, Y. *et al.* Light-avoidance-mediating photoreceptors tile the Drosophila larval body wall. *Nature* **468,** 921–926 (2010).

55. Petersen, L. K. & Stowers, R. S. A Gateway MultiSite Recombination Cloning Toolkit. *PLoS ONE* **6,** (2011).

56. Iyer, E. P. R. *et al.* Functional Genomic Analyses of Two Morphologically Distinct Classes of Drosophila Sensory Neurons: Post-Mitotic Roles of Transcription Factors in Dendritic Patterning. *PLoS ONE* **8,** (2013).

57. Ainsley, J. A. *et al.* Enhanced locomotion caused by loss of the Drosophila DEG/ENaC protein Pickpocket1. *Curr. Biol. CB* **13,** 1557–1563 (2003).

58. Hughes, C. L. & Thomas, J. B. A Sensory Feedback Circuit Coordinates Muscle Activity in Drosophila. *Mol. Cell. Neurosci.* **35,** 383–396 (2007).

59. Song, W., Onishi, M., Jan, L. Y. & Jan, Y. N. Peripheral multidendritic sensory neurons are necessary for rhythmic locomotion behavior in Drosophila larvae. *Proc. Natl. Acad. Sci. U. S. A.* **104,** 5199–5204 (2007).

60. Sweeney, S. T., Broadie, K., Keane, J., Niemann, H. & O'Kane, C. J. Targeted expression of tetanus toxin light chain in Drosophila specifically eliminates synaptic transmission and causes behavioral defects. *Neuron* **14,** 341–351 (1995).

61. Chen, T.-W. *et al.* Ultrasensitive fluorescent proteins for imaging neuronal activity. *Nature* **499,** 295–300 (2013).

62. Gao, Z., Joseph, E., Ruden, D. M. & Lu, X. Drosophila Pkd2 is haploid-insufficient for mediating optimal smooth muscle contractility. *J. Biol. Chem.* **279,** 14225–14231 (2004).

63. Cheng, L. E., Song, W., Looger, L. L., Jan, L. Y. & Jan, Y. N. The role of the TRP channel NompC in Drosophila larval and adult locomotion. *Neuron* **67,** 373–380 (2010).

64. Luo, L., Liao, Y. J., Jan, L. Y. & Jan, Y. N. Distinct morphogenetic functions of similar small GTPases: Drosophila Drac1 is involved in axonal outgrowth and myoblast fusion. *Genes Dev.* **8,** 1787–1802 (1994).

65. Thévenaz, P., Ruttimann, U. E. & Unser, M. A pyramid approach to subpixel registration based on intensity. *IEEE Trans. Image Process. Publ. IEEE Signal Process. Soc.* **7,** 27–41 (1998).

66. Sulkowski, M. J., Iyer, S. C., Kurosawa, M. S., Iyer, E. P. R. & Cox, D. N. Turtle Functions Downstream of Cut in Differentially Regulating Class Specific Dendrite Morphogenesis in Drosophila. *PLoS ONE* **6,** (2011).

67. Iyer, E. P. R., Iyer, S. C., Sulkowski, M. J. & Cox, D. N. Isolation and Purification of Drosophila Peripheral Neurons by Magnetic Bead Sorting. *J. Vis. Exp.* (2009). doi:10.3791/1599

68. Bhattacharya, S., Iyer, E. P. R., Iyer, S. C. & Cox, D. N. Cell-type specific transcriptomic profiling to dissect mechanisms of differential dendritogenesis. *Genomics Data* **2,** 378–381 (2014).

69. Yan, Z. *et al.* Drosophila NOMPC is a mechanotransduction channel subunit for gentle-touch sensation. *Nature* **493,** 221–225 (2013).

70. Zhou, Y., Cameron, S., Chang, W.-T. & Rao, Y. Control of directional change after mechanical stimulation in Drosophila. *Mol. Brain* **5,** 39 (2012).

71. Simone, D. A. in *Encyclopedia of Pain* (eds. Schmidt, R. F. & Willis, W. D.) 412–413 (Springer Berlin Heidelberg, 2007). at <http://link.springer.com/referenceworkentry/10.1007/978-3-540-29805-2_796>

BIOGRAPHY

Kevin Armengol was born and raised in Falls Church, Virginia. Upon graduation from Bishop Dennis J. O'Connell high school in 2007, he went on to receive his B.A. in Cognitive Science from the University of Virginia. Before attending George Mason University, Kevin spent a year working as an emergency room scribe. In his free time he likes to read, play sports, and create music.